Nélida Sofia Tavares Furtado

Licenciatura em Ciências
da Engenharia Química e Bioquímica

Ageing on commercial automotive catalysts, a structure reactivity study

Dissertação para obtenção do Grau de Mestre em
Engenharia Química e Bioquímica

Orientador: Patrick da Costa, Professor, UPMC.
Co-orientador: Mário Eusébio, Professor Auxiliar, FCT.

Júri:

Presidente: Professora Doutora Maria Dionísio Andrade
Arguente: Professora Doutora Isabel Fonseca
Vogal: Professor Doutor Mário Eusébio

FACULDADE DE CIÊNCIAS E TECNOLOGIA
UNIVERSIDADE NOVA DE LISBOA

Novembro 2014

Ageing on commercial automotive catalysts, a structure reactivity study

Dedico esta tese à minha família,

em especial às mulheres de força e coragem que a constituem,

aos meus amigos e a ti Milo.

Abstract

Increasingly stringed regulations for diesel engine emissions have a significant impact on the required efficiency of DOC. Lowered DOC oxidation efficiency due to thermal aging effects influences the efficiency of the exhaust aftertreatment systems downstream of the DOC. In this work carried out in the Jean Le Rond d'Alembert Institute the effect of hydrothermal aging on the reactivity and structure of a commercial DOC was investigated. The characterization of the catalytic performance was carried out on a synthetic gas bench using carrots catalyst under conditions close to the realistic conditions i.e. using a synthetic gas mixture, representative of the exhaust gases from diesel engines. Different structural characterization techniques were performed: textural and morphological proprieties were analyzed by BET and TEM, the characterization of the presented crystallographic phases was performed by DRX and the determination of the number of reducible species was possible by TPR. TEM results shown, an increase of the metal particle size with the aging caused by the agglomeration of metal particles, revealing the presence of metal sintering. DRX results also suggest the presence of support sintering. Furthermore, DRX and BET results unexpectedly reveal that the most drastic aging conditions used actually activated the catalyst surface. As expected, the aging affected negatively the catalyst performance on the oxidation of methane and CO, however an improvement of the NO oxidation performance with the aging was observed. Nevertheless, for the aging conditions used, catalytic activity results show that the influence of aging in DOC performance was not significant, and therefore, more drastic aging conditions must be used.

Keywords: diesel exhaust oxidation catalyst; hydrothermal aging; synthetic gas bench; structure characterization; methane oxidation

Resumo

Regulamentações cada vez mais rígidas para as emissões de motores a diesel tem um impacto significativo na eficiência exigida ao DOC. A baixa eficiência de oxidação do DOC devido ao envelhecimento térmico influencia a eficiência dos restantes componentes do sistema de tratamento de gases à jusante do DOC. Neste trabalho, realizado no instituto Jean Le Rond d'Alembert o efeito do envelhecimento hidrotérmico na reactividade e na estrutura de um DOC comercial foi investigado. Os ensaios catalíticos foram efectuados num banco de gás sintético utilizando condições próximas às condições reais, isto é, utilizando uma mistura de gás sintético representativa dos gases à saída de um motor a diesel. Diferentes técnicas de caracterização estrutural foram utilizadas: as propriedades texturais e morfológicas foram analisadas por BET e TEM, a caracterização das fases cristalográficas presentes foi efectuada através de DRX e a determinação do numero de espécies reduzidas foi possível através de TPR. Os resultados do TEM mostram um aumento no tamanho das partículas metálicas com o envelhecimento, ou seja, revelam a presença de sinterização de partículas. Os resultados do TPR indicam ainda a possível presença de sinterização do suporte. Ao contrário do esperado, os resultados de DRX e BET revelaram que as condições de envelhecimento mais drásticas activaram a superfície do catalisador. Como esperado, o envelhecimento afectou negativamente a eficiência do catalisador na oxidação do CH_4 e CO, enquanto, para o NO houve um aumento da oxidação com o envelhecimento. Apesar disso, conclui-se que para as condições de envelhecimento utilizadas a influência do envelhecimento na eficiência do catalisador foi pouco significativa e, por conseguinte condições mais severas de envelhecimento deverão ser utilizadas.

Palavras chave: DOC; envelhecimento hidrotérmico, banco de gás sintético, caracterização estrutural; oxidação de metano.

Index

Table of Contents

Figures Index

Table Index

Abbreviations Index

DOC: Diesel Oxidation Catalyst

TEM analysis: Transmission Electron Microscopy

TPR analysis: Temperature Programmed Reduction

BET analysis: Brunauer, Emmet and Teller

DRX analysis: X-ray Diffraction

SGB: Synthetic Gas Bench

Chapter 1: Introduction and Objectives

This work was carried out in the Jean Le Rond d'Alembert Institute of Pierre and Marie Curie University, in cooperation with Continental with the purpose of researching the effect of aging on diesel oxidation catalysts, and will be used to control the emissions of pollutants of vehicles in Europe.

The widespread use of automobiles offers a degree of mobility to the individual that was unthinkable just a few centuries ago, additionally it gave an important contribution to the development of our modern society [1] [2]. On the other hand, the inherent consequences are evident: in 2010, over 1 billion passenger cars were on the streets worldwide [3] ,and 63 million additional new cars were produced in 2012, being 17 million produced in Europe (2nd world largest producer) [4].

This enormous number of vehicles indicates that there are several severe problems one has to deal with me. Almost all cars are powered by combustion engines which are fuelled by gasoline, diesel or natural gas, and therefore rely upon fossil fuels. These natural resources are limited and must be conserved. Tremendous efforts are made to limit the wastage of this raw material. Manufactures are urged to offer cars with economical engines, and the government tries to motivate the drivers to buy electric vehicles through fiscal incentives. A lot of research is done to establish new engine concepts based on renewable energies (fuel cell technology, hydrogen engines, etc.) instead of conventional petrol driven cars. But until these new technologies are fit for series-production, the existing automotive combustion engines have to be improved and optimized to use the existing fuel resources responsibly [5].

Furthermore, there is an increasing ecological consciousness to protect our natural environment. The combustion of fossil fuels in millions of cars produces large amounts of gaseous emissions, emerging as the major source of urban air pollution in the developing world

In order to preserve air quality, the European Union (UE) issued in 1970 its first directive (Directive 70/220/EEC), also known by Euro 1, regulating the maximum quantities of pollutants that can be emitted by an automobile vehicle, so that it can be approved for sale in UE [6]. Since then, successive "Euro" norms have been introduced imposing more stringent limits for the emissions of different pollutants and in the long run further lowering can be expected. The commonly controlled gas emissions are carbon monoxide (CO), hydrocarbons (HC), oxides of nitrogen (NOx) and particulates (for diesel engines).

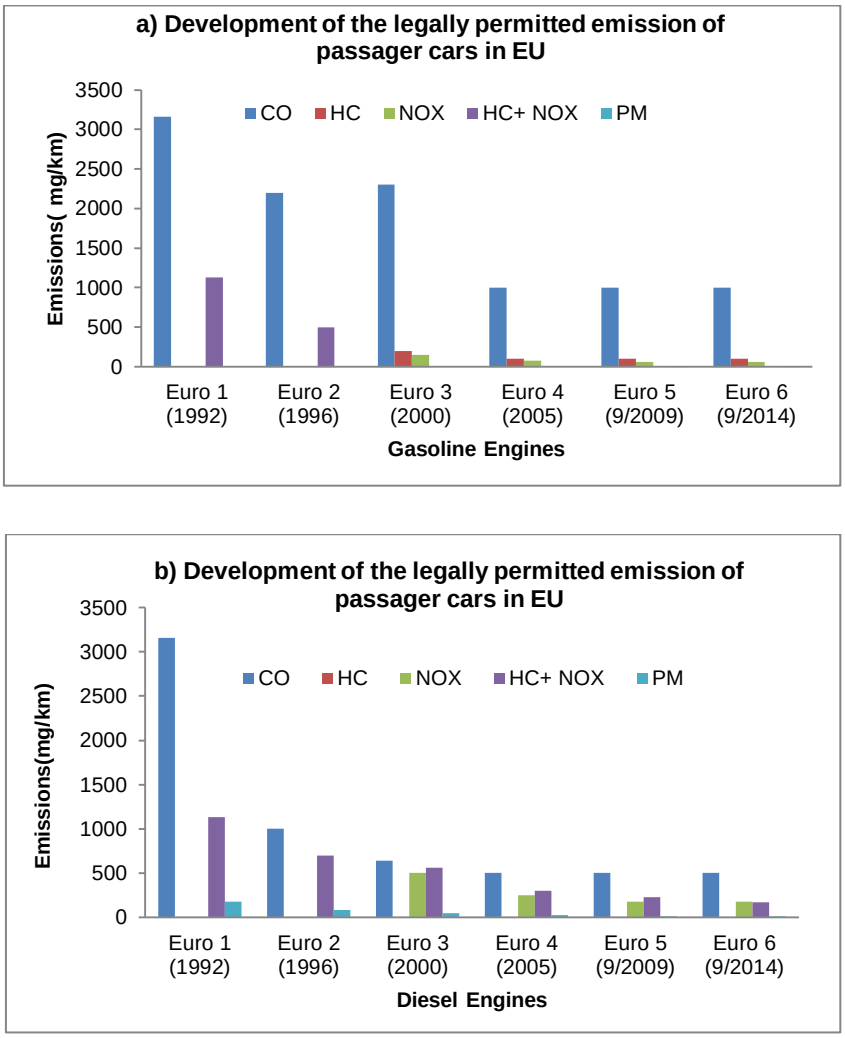

Figure 0.1 - Development of the legally permitted emission of passenger cars in EU a) For gasoline engines b) For Diesel Engines

The need to respond to government legislation to reduce emissions from vehicles, like Euro 5 and further Euro 6, places increasing demands on the automotive industry to seek improvements in automotive emission control systems enclosing new engine concepts, fuel quality, and in the design of exhaust catalysis, therefore they are currently spending a lot of money on research on these fields [5] [7].

Particularly, the continuous improvement of exhaust catalysts over the last 30 years brought major advances in saving resources and fluffing present and further emissions directives. It is estimated that by the year 2000, over 800 million tons of combined pollutants of HC, CO and NO*x* could have been abated using auto exhaust catalyst. Nevertheless, there is still a need for further improvement of automotive catalyst technology, to meet the legal standards, as well as to minimize the pollutants toxic to the human health and prejudicial to the environment [5].

Although there are many variations, catalytic converters can be grouped into two main categories. The first category is comprised of the system used for engines that have stoichiometric air to fuel ration. These engines are usually spark ignition engines. Catalytic converters of this type use a three way catalyst (TWC), in which the three pollutants (CO, HC and NOX) are simultaneously reacted to eliminate them all. In the second category are systems for engines operated with excess oxygen (lean burn) such as compression ignition diesel engines.

For these systems, due to the high concentration of oxygen in the exhaust gas, it is impossible to reduce NOx over a TWC. To overcome this problem, a combination of two types of converters in series is used: on for oxidation and the other for reduction. The first one, called diesel oxidation catalyst (DOC) is responsible for oxidizing CO and HC. In this converter, NO is also oxidized to NO_2, although some nitrous oxide (N_2O) and nitrogen (N_2) can also be formed through selective catalytic reduction.

A diesel particulate filter (DPF) is placed after the DOC to trapsoot, which can be subsequently oxidized by NO_2 produced in the DOC. The second converter, either a selective catalytic reduction unit (SCR) or a lean NOx-trap (LNT) is used to convert NO and NO_2 to nitrogen using a reducing agent -urea/water solution (UWS). Sometimes the DPF and SCR functions are combined. The reduction of NOX in the SCR depends on the ratio of NO to NO_2, thus the extent of NO oxidation in the DOC is important. Finally, an ammonia slip catalyst may be used to eliminate excess ammonia fed to an SCR.

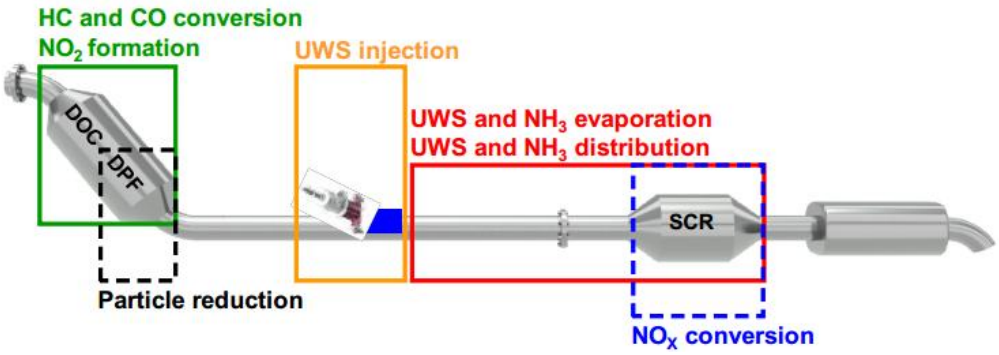

Figure 0.2 - Components of an abatement system. Reproduced from [8].

Currently, the SCR and the lean NOx trap are reserved for the heavyweight vehicles and commercial vehicles, but with implementation of Euro 6 legislation, that focus mainly in the reduce of nitrogen oxide emissions, all diesel cars must implement one of these technology's [9].

A lot of interest is currently focused on catalysts for emission control in diesel engines, since diesel engines enjoy increasing popularity, due to their economy of operation and their reduced emission of greenhouse gases, most notably CO_2 [5] [10].

According to [11], the vast majority of Europe's new cars are powered by gasoline or diesel motors: diesel cars account for 55% of all new registrations, gasoline cars for 42%; all other technologies – hybrids, electrics, and natural gas and ethanol-fuelled vehicles – combine to make up the remaining 3% (Figures of 2013).

Increasingly stringed regulations for diesel engine emissions have a significant impact on the required efficiency of DOC, which has to convert more pollutants at lower temperatures. Measures to reduce engine-out NOx and PM, tend to increase CO and HC emissions. Additionally, engine-out NOx reduction is mainly achieved through high amounts of exhaust gas recirculation (EGR) that lower the combustion temperature,which impose great challenges to tradional diesel oxidation aftertreatment devices.

Chapter 2: Context of the bibliographic study

In this chapter the context in which this study was carried out will be presented. This chapter can be divided in 4 main sections.

The first one, where the components of diesel exhaust emission and their treatment are presented. The second one, where diesel oxidation catalysts (DOC) is discussed in general. In the third section, the main topic of this study - ageing of DOC- is primarily discussed. The last section covers several topics that are important for global comprehension of the study.

2.1. Diesel exhaust emission

Engine exhausts consists in a complex mixture, which composition depends of a variety of factors such as: type of engine (two- or four-stroke, spark-or compression (diesel)-ignited), driving conditions, e.g. urban or extra-urban, vehicle speed, acceleration/deceleration, etc. Diesel engines and lean-burn gasoline engines became more and more important due to current efforts to increase fuel economy and reduce emissions of the greenhouse gas CO_2 [12].

Diesel exhaust is lean because the engine only injects the required amount of fuel into compressed hot air to generate the desired power. Partly due to the excess air input, diesel exhaust is also, typically lower in temperature and have less NO*x* than gasoline exhaust. Diesel and lean-burn gasoline engines are more fuel efficient, and other benefits include lower CO_2 production and for diesel engines specifically, higher power production and durability.

However, of the combustion process result larger quantities of unburned fuel, lubricating oil emissions and soot and the higher air-to-fuel ratio (fuel-lean, oxygen-rich environment) makes the reduction of NOx to N_2 more difficult. A trade-off between particulates and nitric oxides impedes the simultaneous reduction of both emissions [1].

Diesel engines, due to their comparatively lean-burn characteristics produce, besides gaseous compounds, liquid and solid combustion products [12]:

- Solid: dry carbon or soot;
- Liquid: unburned fuel, lubricating oil (collectively SOF) and liquid sulphates primarily, sulphuric acid (H_2O associated with the SO_3 is included as a component of the liquid particulate);
- Gas: carbon monoxide (CO), hydrocarbons (HC) derived primarily from partially burned fuel, oxides of nitrogen and sulphur.

2.2. Pollutant formation and treatment

In a combustion engine a hydrocarbon fuel is oxidized by atmospheric oxygen. Under ideal conditions only CO_2, water, and heat would be generated (1).

$$C_mH_n + (m + 0.25n)O_2 \rightarrow mCO_2 + 0.5nH_2O \quad \textbf{(2.1)}$$

Under engine conditions, however, ideal combustion is impossible because of the lack of chemical equilibrium and the inhomogeneous gas phase. Therefore, besides water and carbon dioxide, several other components, result of incomplete combustion, are found in the exhaust gas [12].

The challenge for the automobile industry is to remove from these exhaust gases components that have environmental and health implications, as greenhouse effect and urban smog. Nowadays these components are [13] [9].

- **Carbon monoxide (CO):**

Carbon monoxide is a colourless and odourless gas, formed as an intermediate reaction product during combustion of hydrocarbons. Incomplete combustion due to low combustion temperature, lack of oxygen, or too short reaction time leads to the emission of CO, a poisonous gas that displaces oxygen from the blood.

- **Unburned and partially oxidized hydrocarbons(HC)**

Incomplete combustion of hydrocarbon fuels leads to the emissions of unburned and partially oxidized hydrocarbons. The hydrocarbons emitted from internal combustion engines are always a mixture of various compounds: paraffins, olefins, acetylenes, and aromatics. The composition depends on the combustion system, the operating conditions of the engine, and the fuel. The known effects of hydrocarbons for the human health are related with the carcinogenic and mutagenic caused by benzene and other aromatics.

- **Oxides of nitrogen (NO*x* : *NO+*NO_2)**

They are generated at combustion temperatures by oxidation either of atmospheric nitrogen or nitrogen contained in the fuel. During the combustion process mainly NO is formed; NO2, which is more toxic than NO, is formed by the relatively slow oxidization of NO in the atmosphere. In combustion processes with an excess of air significant NO_2 can be expected. NO*x* also reacts with hydrocarbons in sunlight to form ozone and photochemical smog. NO*x* can increase respiratory illnesses and is a contributor to acid rain. Tropospheric ozone causes breathing difficulties and damages plants. In the upper atmosphere NO*x* is involved in a catalytic cycle that leads to the destruction of the ozone layer.

- **Particulate Emissions(PM)**

Particulates are tiny solid and liquid particles. They occur in the exhaust of diesel engines in sizes from 0.01 to 1 µm and consist of carbon-rich particles (soot), hydrocarbons, and sulphates. In a diesel engine, due to incomplete mixing, zones of air deficiency arise and lead to soot formation. In parallel, in zones with excess air, soot is partially burned.

Recent research has shown that especially ultrafine particles (<100 nm in mean diameter) and nanosized particles (<50 nm in mean diameter) are potentially dangerous due to their capability to enter deep into the respiratory tract. Furthermore, these small particles supposedly can penetrate cell membranes.

Noteworthy, that carbon dioxide (CO_2), although the most commonly emitted combustion gas, is normally not considered as a pollutant since adverse health effects are not known. However, CO_2 should be regarded as a serious pollutant in terms of its global-warming potential.

The basic reactions for CO and HC in the exhaust are oxidation with the desired product being CO_2, while the NOx reaction is a reduction with the desired product being N_2, and the particles are treated by combustion of suit in CO_2. A catalyst promotes these reactions at lower temperatures than a thermal process.

2.3. Diesel oxidation catalysts

The diesel oxidation catalyst (DOC) has been part of diesel exhaust systems since regulations were introduced to limit the amount of harmful emissions released to the environment from diesel engines .The DOC primary functions are oxidation of CO, unburned hydrocarbons to less harmful products CO_2 and H_2O (2-3) and NO to NO_2 (4) , which is important for efficient performance of various downstream catalysts, such as NOx storage/reduction (NSR) catalysts, SCR catalysts and DPFs (further discussed below). DOC has also the additional role of periodically converting high amounts of HC and CO to generate the required thermal conditions to burn the soot trapped in the DPF [14].

$$CO + \frac{1}{2}O_2 \rightarrow CO_2 \quad \textbf{(2.2)}$$

$$HC + O_2 \rightarrow CO_2 + H_2O \quad \textbf{(2.3)}$$

$$NO + \frac{1}{2}O_2 \rightarrow NO_2 \quad \textbf{(2.4)}$$

The first support for oxidation catalysts in automobiles was pellets in a canister, or a packed bed arrangement, nevertheless this support was put aside due to the dramatic decrease in catalytic performance over time caused by the mechanical degradation of the pellets via vibration and inter-particle collision.

Current DOCs are generally based on cordierite (ceramic) “honeycomb” monoliths although metal monoliths are also sometimes used. The ceramic monoliths have superior strength due to the low porosity of the ceramic; however this property makes the monolith unsuitable to disperse the catalyst. As such, a high surface area material, called a washcoat, is adhered to the monolith surface, and the catalytic metal is then dispersed on the washcoat.

Using a high surface area washcoat support results in highly dispersed precious metal sites, which is generally desired for good oxidation performance, because it increases the active component exposed surface area for reaction and also lowers the amount of precious metal required, thus decreasing the catalyst cost [1].

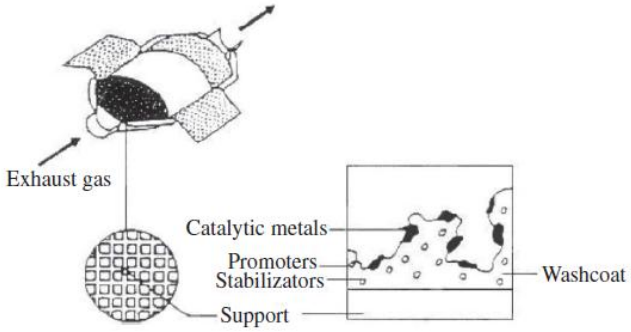

Figure 1.1 - The structure of a monolithic exhaust gas catalyst. Reproduced from [1]

Alumina (Al_2O_3) is a very common washcoat material, among others like silica (SiO_2) and zeolites, as well as combinations of these components. Noteworthy is that each material has different properties that will affect its application and these properties can be tailored for the target reactions. This can be explained if we consider the fact that catalyst support can influence performance, for example by altering the thermal stability of the active component and support, surface area, pore volume and surface reactivity. Examples of several experiments that corroborated this can be found in [1].

Some supports additives have been used to improved thermal stability of the support. Typically, the additives for Al_2O_3 are metal oxides such as BaO, CeO_2, La_2O_3, SiO_2 and ZrO_2, although these components can have other, possibly undesired (such as active site blocking), effects on catalyst activity and therefore must be evaluated carefully [1].

As for the active components, Platinum group metal, including Platinum (Pt) and Palladium (Pd) have been used in DOCs since their inception due to their good oxidation performance, their good thermal durability, their lower tendency (compared with transition metals) to react with support materials and they can process gas streams containing upwards of 1000 ppm (by weight) sulphur without being transformed to bulk surface. Additionally Rhodium (Rh) is sometimes used as well [15] [1].

However, in early R&D on automotive catalysts, it was attempted to use transition metals, such as, copper and nickel largely due to concerns over the cost and availability of noble metals. Nevertheless, it quickly became apparent that transition metals lacked intrinsic reactivity, thermal durability and fuel oil contaminants (poison) resistance required for automotive applications [15].

In terms of diesel emissions, DOCs with precious metal components provide high oxidation activity for CO, unburned hydrocarbons, and liquid hydrocarbons (SOF components) [1].

The advantages and disadvantages of using Pt or Pd as active components are briefly discussed below: while both metals act as adsorption sites for both oxygen and HCs, Pt has lower relative surface oxygen coverage and is stereotypically considered to have the highest oxidation activity. Pt also exhibits better performance with higher weight HCs compared to Pd. Where extreme temperatures are not required, Pt provides good oxidation activity and sufficient activity in the presence of SO_2, a common catalyst poison.

However, in terms of thermal degradation, i.e., when high temperatures exist such as those generated in the DOC for DPF regeneration, Pt activity decreases due to thermal degradation. Similarly, Pd-based catalysts are also deactivated by high temperature exposure, which can cause sintering (that will be discussed on section 2.5), and decomposition of the active PdO to metallic Pd (that is less active), thereby decreasing catalyst activity. The associate use of Pt and Pd (that will be mention more in detail on section 2.5) has shown more resistance to sintering at higher temperatures than Pt [1].

A highly dispersed state is desired for the metal, as activity generally increases and cost decreases with the surface-to-bulk (higher surface area for reaction) ratio of the particles, although there is a lower limit on particle size for good oxidation performance [1].

2.4. Catalyst Deactivation

Catalyst deactivation, the loss over time of catalytic activity and/or selectivity, is a problem of great concern in the practice of industrial catalytic process. Catalyst deactivation may occur by several mechanisms, nevertheless the most relevant mechanisms are sintering (also known by aging), fouling/coking and poisoning. These mechanisms can be classified according to their nature in chemical, mechanical or thermal. A brief description of each mechanism is presented in Table 2.1.

Table 1.1 - Mechanisms of catalyst deactivation [16]

Mechanism	Type	Brief Description/Definition
Poisoning	Chemical	Strong chemisorption of species on catalytic sites, thereby blocking sites for catalytic reaction
Fouling	Mechanical	Physical deposition of species from fluid phase onto the catalytic surface and in catalyst pores
Sintering (Aging)	Thermal	Thermally induced loss of catalytic surface area, support are and active phase-support reactions

While catalyst deactivation is inevitable for most processes, some of its immediate drastic consequences may be avoided, postponed or even reversed, therefore there is considerable motivation to understand and treat catalyst decay. This area of research provides a critical understanding which is the foundation for a modeling deactivation processes, designing stable catalysts and optimizing processes to prevent or slow catalyst deactivation [16] . In this work only the aging mechanism and their effect on catalytic activity for diesel oxidation catalyst will be discussed.

Since the study of deactivation is usually conducted with synthetic aging, which attempts to simulate the effects of actual aging in a shorter time frame and for less cost, it's important to find correlations between real and simulated for the development and assessment of catalysts. Differences can arise between the aging methods, i.e. physical aspects of aging; take for example the different effects observed on Pt/Al_2O_3 using homogeneous or heterogeneous thermal aging.

For a homogeneous thermal aging process, where the catalyst was aged in an oven at 675ºC, the time for the back-to-front ignition wave to travel increased through the entire catalyst length compared to the fresh catalyst sample, and the aged catalyst dispersion measured by H_2 chemisorption was 42% of the fresh catalyst dispersion [17].

While for the heterogeneous/non-uniform aging method, damaged wasn't uniform through the catalyst, i.e. each axial position of the catalyst of the catalyst was exposed to a different thermal aging temperature environment, with higher temperature exposures at the catalyst inlet.

This was achieved pulsing propylene and oxygen into the reactor at 500ºC, resulting in the inlet section of catalyst experiencing temperatures above 650ºC, thus indicating Pt sintering. Additionally and despite the similar increasing on the back-to-front ignition time, the time increase was focused heavily toward the catalyst inlet [18].

2.5. Aging of catalysts

The nature of automotive applications demands reliable performance of catalytic converters over an extended time period with transient operating conditions. To achieve that, one of the key challenges is dealing with the chemical and thermal aging effects on the catalytic activity. In this work only thermal aging is predominantly discussed.

Being the first component exposed to "fresh" diesel exhaust, the DOC experiences more damage than downstream components and besides that, new exhaust emission regulations have a particular impact on the conditions of operation of DOC.

For example, active regeneration of diesel particulate filters (DPFs) by soot burning requires the DOC withstand high temperature spikes. These exceed by far comparatively low diesel exhaust gas temperature, thus causing potential thermal aging issues. Furthermore, with new regulations limiting the sulfur content in diesel to 10 ppm, the same level as in gasoline, the influence of motor oil based contaminants (e.g. Zn, Ca, Mg, P, Si) on the chemical aging of the DOC is likely increase. Additionally, diesel can contain additives like ferrocene (Fe) used for improved DPF regeneration, which can also contribute to chemical aging [19].

It's important to mention, that the exhaust conditions affect the type and extent of deactivation. Driving behavior has also been seen to impact the deactivation of catalysts, with highway driving leading to more thermal deactivation and city driving with idling causing more poison accumulation. Thermal aging tends also to increase with mileage, as the precious metal dispersion decreases with aging time [1].

Lowered DOC oxidation efficiency due to aging effects can lead to reduced NO_2 formation. This potentially influences the efficiency of the exhaust aftertreatment systems downstream of the DOC, including the diesel particulate filter, the NOx storage reduction catalyst, and the selective reduction catalyst.

The DPF employs NO_2 as an oxidizing agent to remove trapped soot; a lowered NO_2 concentration can lead to blockage of the DPF. Besides that, DPF require temperatures of about 500-600°C to oxidizes diesel particulate matter (soot) with O_2.

However, NO_2 oxidizes soot at temperatures close to 350°C. An NSR catalyst selectively stores NOx during lean-phase operation (excess of O_2) and reduces this stored NOx through a short, reductant - enriched (rich) phase.

Several studies have proposed that NO_2 is a precursor for, or intermediate in the trapping process and overall, the presence of NO_2 enhances the performance of the NSR catalyst through improved NOx storage SCR catalysts selectively reduce equi-molar concentrations of NO and NO_2 to N_2 in the presence of NH_3 at faster rate than if only NO was available. [19]. NSR catalyst can only store NO_2 but not NO; lowered NO-oxidation efficiency of the DOC can therefore result in NO slip

2.5.1. Thermal aging or Sintering

Sintering is a physical process where the active surface area of the catalyst decreases through structural changes. It occurs, unequally, to both the catalyst support and active metal sites, based on the exhaust gas conditions. However, temperature has the greatest effect on the degree of sintering, with more sintering occurring as the temperature increases and with the length of temperature exposure [1].

2.5.1.1. Support Sintering

As mentioned before alumina is the most common washcoat material for DOC, however there are many different types of alumina. High temperature exposures cause undesired phase transformations for alumina that change the washcoat properties: y-Alumina, having a high surface area(a strong desired property for the catalyst support), is gradually transformed to δ-Alumina and at still higher temperatures to α-phase via Θ-phase. [1] [20].

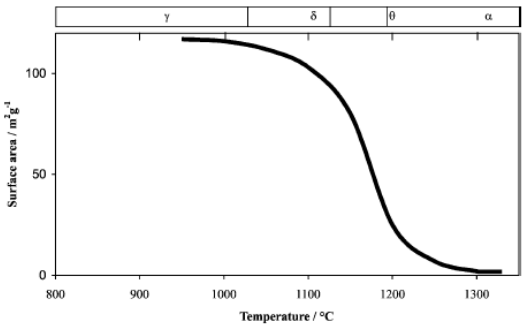

Figure 1.2 - Phase transformation and specific surface are of alumina. Reproduced from [20]

The driving force for sintering is to lower the surface energy of the support, which occurs through the transport of the material across the surface to decrease dispersion and/or eliminate pores in the support. The result of support sintering in catalysts is the loss of surface area of the carrier (or the washcoat in case of structured catalysts), besides that when the pores are blocked off, the precious metal particles can be trapped inside (encapsulation) and hidden from the reactants thereby decreasing the overall catalyst activity [1] [20].

Particle growth occurs by successive elimination of water via condensation of hydroxyl groups residing on adjacent particles close to an area of contact. The formed Al-O-Al bond brings more hydroxyls into adjacency and in such way results in closure of pores [20].

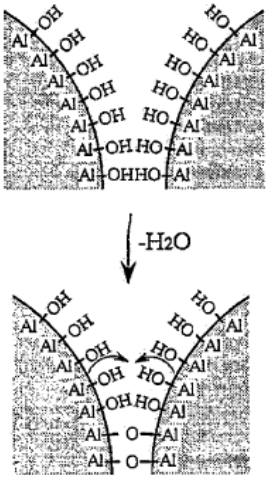

Figure 1.3 - A model representing surface dehydroxylation from contact region of two adjacent particles. Reproduced from [20].

Temperature, size and shape of the metal particles, as well as roughness, reaction atmosphere, metal type, metal dispersion, promoters/impurities and support surface are used are the main parameters controlling the sintering of given oxide [1] [20] [16]. However, temperature has the greatest effect on the degree of sintering, with more sintering occurring as the temperature increases and with the length of temperature exposure [1].

An example regarding reaction atmosphere, is the fact that water vapor accelerates the crystallization and structural change in oxide supports [20] .

In a study of water deactivation of PdO catalyst, Burch and Urbano [21] suggested the active sites become more mobile on the catalyst surface which causes decreased activity for PdO active sites; the water, or the surface hydroxyl group interactions, allows the PdO to travel more easily over the alumina washcoat. In the same study the investigators observed that the long duration hydrothermal aging step caused permanent damage on the catalyst, possibly due to Pd oxides changing to less active state. Other study [22] showed that a higher HC oxidation light-off temperature over Pt- zeolite catalysts following hydrothermal damage, as well as a lower surface area for both zeolite alone and Pt-zeolite combination, indicating that the zeolite support is damaged.

2.5.1.2. Precious metal sintering

Precious metal sintering generally involves the movement of precious metal particles, allowing agglomeration of the particles, and thus decreasing both the dispersion of the metal on the surface and the surface-to-volume ratio of the particles [1]. Two sintering models have been proposed for washcoat-supported precious metal catalysts, namely atomic and crystallite migration models. In the first model, sintering occurs via escape of metal atoms from crystallite and is transferred across the surface. Collision of these migrating atoms with other metal crystallites results in the formation of larger particles. Based on the crystallite migration model, sintering is taking place via migration along the support surface. The collision and coalescence of two crystallites leads to the formation of larger particles. [20]

Calcium, barium and cerium are known to decrease the mobility of the atoms. Rare earth oxides such as La_2O_3 and CeO_2 are strongly interacting with noble metal particles to improve support stability and thus reducing the sintering of some metals, although not Pt in particular.

As discussed above, blends of precious metals, such as Pt-Pd, have exhibited more resistance to sintering compared to monometallic catalysts. The addition of Pd improved the DOC thermal stability by mitigating the growth of precious metal particles, possibly because a portion of the Pd forms a protective Pd oxide (PdO) layer [1].

2.6. Influence of different parameters on the light off (ignition) curves

2.6.1. Influence of the type of catalyst (Pd vs Pt:Pd catalyst) on the ignition curve of propene

Khosravi et al. [23] study the oxidation of CO, NO and C_3H_6 and reduction of NO by propene over DOCs using two commercial monolith samples of 400 CPSI with the total PGM loading of 95 g/ft^3, one monolith had platinum catalyst only and the other was a bimetallic catalyst of 4:1 by mass platinum and palladium. For the Pt catalyst, the investigators obtained ignition curves similar to reported on the literature, i.e. the oxidation of CO occurs first, followed by that of C_3H_6. As the propene begins oxidizes, it reacts with NO to produce N_2 and N_2O, and finally NO is oxidized to NO as the C_3H_6 vanishes (Figure 2.4a).

However for the Pt:Pd catalyst there is a different shape for the propene ignition curve. It is divided into two distinct regions, with a noticeable change in slope, and in some cases a plateau, in the conversions between them (Figure 2.4b). Noteworthy is also the fact, that this behavior was not seen for the same conditions in the absence of CO. From an examination of these results, the investigators suggested that the slope change of the propene ignition tended to happen at the point where the outlet CO conversion was close 100%.

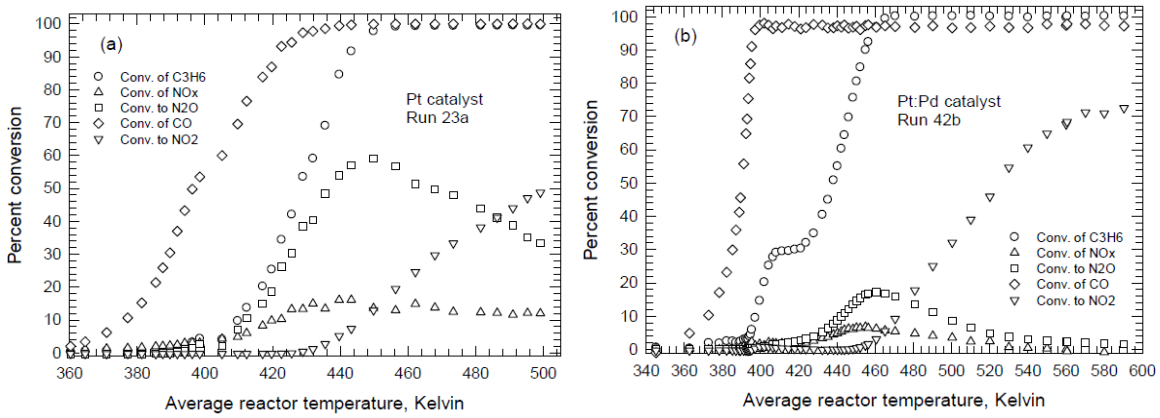

Figure 1.4- Typical ignition curves observed for the complete exhaust gas mixture over two catalysts. a) Mono-metallic Pt catalyst: 500 ppm CO, 167 ppm H_2, 500 ppm propene, 150 ppm NO b) bi-metallic Pt:Pd catalyst: 500 ppm CO, 167 ppm H_2 , 500 ppm propene, 600 ppm NO. Reproduced from [23].

2.6.2. Influence of variation of the concentration of CO and NO in the ignition curve of propene

In the same study [23] the investigators also observed that the shape of the propene curve depend on the feed concentration.

They found that when increasing the concentration of CO, keeping the remaining feed concentrations constant, the conversion of NO is essentially the same, including the product distribution, while the ignition curve of CO has moved to the right, as expected due to its self initbition. As for the C_3H_6 ignition curve, they observe a change of slope and they noticed that that change coincides with the point of complete CO conversion at the reactor outlet (Figure 2.5).

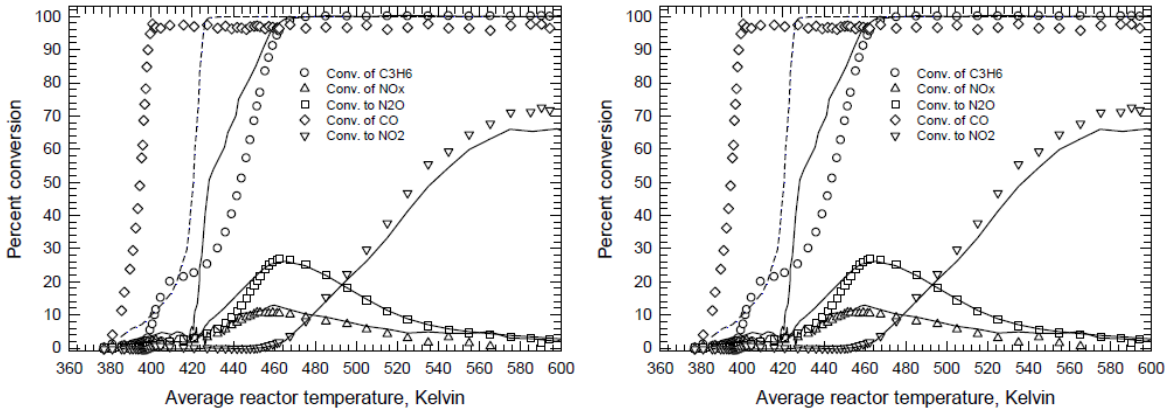

Figure 1.5- Effect of increasing the concentration of CO. Both experiments used 750 ppm propene and 600 ppm NO, but the CO concentrations were 500(represented by symbols) and 2000 ppm (represented by lines). The dashed line is the CO conversion for the experiment with 2000 ppm CO. Reproduced from [23].

Moroever, the authors observe that increansing the NO concentration causes a sharper deviation with concominant flat area on the shape of the propene oxidation curve. The investigators also highlighted that the increase of NO concentration supressesed the catalytic reduction of NO, while the conversion to NO_2 remained essentially the same.

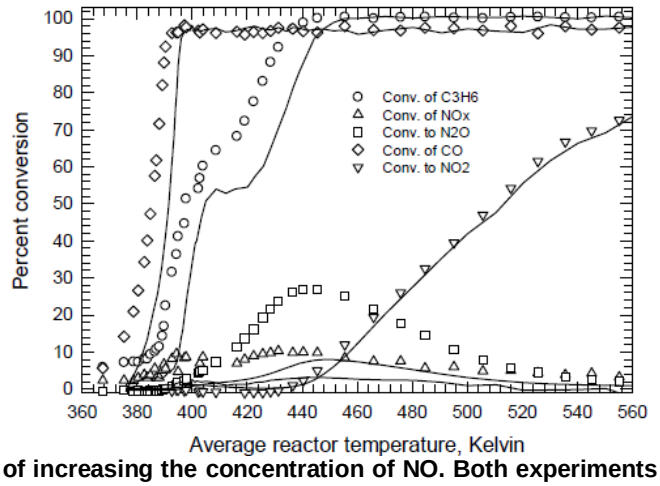

Figure 1.6- Effect of increasing the concentration of NO. Both experiments used 250 ppm propene and 500 ppm CO, but with NO concentrations of 150(represented by symbols) and 600 ppm (represented by lines). The higher NO concentration causes a sharper deviation with concomitant flat area. Reproduced from [23]

In another study [24] the authors found that the addition of NO caused propene oxidation light off to occur at higher temperature, resulting in less propene conversion across the entire temperature range, in comparison to experiments without NO (Figure 9 of [24])

In the same study by [24], the influence of NO_2 on the light off curve of propene was also studied. The authors observed that although propene oxidation light off occurred at the same temperature when NO_2 was or was not included, the addition of NO_2 initially accelerates the C_3H_6 oxidation, relative to no NO_2, but then inhibits it after light off has occurred. The authors attribute this negative effect to NO inhibition of C_3H_6 oxidation reaction, with the NO formed from NO_2 reduction.

2.6.3. Influence of variation of concentration of HC in the ignition curve of NO

Karishma and al [24] investigated the effect of HC species on NO oxidation over Pt-Pd catalyst and observed that under the conditions of the study , increasing amounts of C_3H_6 resulted in lower NO oxidation conversion, due to the consumption of product NO_2 as an oxidant in C_3H_6 oxidation (Figure 2.7).

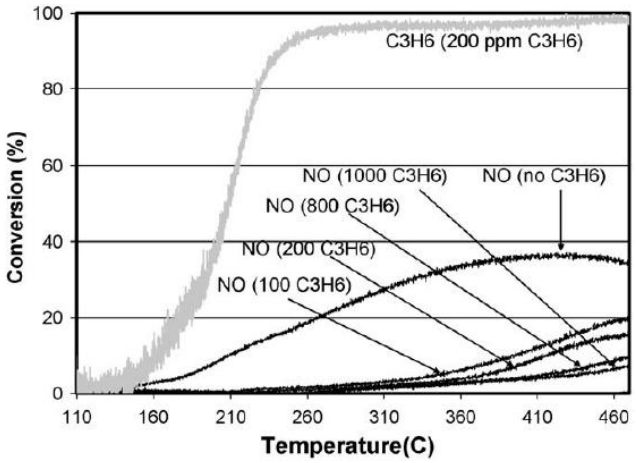

Figure 1.7- NO and propene oxidation conversion as a function of temperature and propene concentration. The feed stream contained 200 ppm NO, 10% O2, 5%H2O and either 0,100, 200, 800 or 1000 ppm propene, and a balance of N2. Reproduced from [24].

These mechanism of inibhition was also reported in a earlier study [25], where the authors showed that with aged DOCs, reductants can facilitate the complete reduction of product NO_2 back to NO. The authors conclude that once all the reductants were consumed did the NO oxidize back to NO_2. These findings indicated that for aged DOCs, as long as HC and CO are present in the exhaust, NO_2 can be consumed by the DOC, thus hindering the performance of the downstream devices.

In the same study the authors [24] also investigated the influence of the different species of HC on NO_2 reduction by HC, using equivalent C:N ratios. They observed that NO_2 reduction by C_3H_6 starded at a lower temperature than that observed with $C_{12}H_{26}$ and m-xylene, whereas with these two larger molecules similar results were obtained. This demonstrates that the NO_2 reduction by HC is dependent on the type of HC itself.

Additionnaly different C_3H_6 concentrations were used to investigate the impact of HC concentration on NO_2 reduction. With every increase in the propene concentration, in the range examined, reduction began at a lower temperature and the extent of NO_2 reduction increased as well. Futhermore, as more C_3H_6 was added, the temperature range across which reduction occurred became smaller. These data show that the temperature where HC oxidation via NO_2 begins it's also dependent on the amount of HC present.

2.7. Zone Coated Catalysts

The achievement of tigher emission standarts relies also on the reduction in the cold-start emissions by attaining faster light-off of the catalytic converter, since automotive catalysts operate inefficiently until they reach their light off temperature.

To improve the light-off performance and conversion of catalytic converters, the effect of variatious design factores (such as cell density, length and diameter of the monolith, composition of catalyst and axial catalyst distribution) on the performance of the catalyst converter has been extensively study . Non-uniformly distributed metal or zone coated catalysts has been receiving a particular interest from investigators [26].

For DOCs, the premise is that different Pt loadings would be used for different axial sections of the catalyst to minimize the total amount of Pt used while still meeting emissions targets for NO, CO, and/or HC conversions and possibly improving cold-start emissions [1] .Many researches ([27], [28], [29]) investigate this concept with models and their studies indicate that non-uniform catalyst distribution can improve the performance of catalytic converter. Oh and Oh and Cavendish [28] examined the light-off behavior of three Pt distribution profiles along the reactor length and showed that light-off performance improves substantially when the noble metal is concentrated in the upstream section of the monolith. Cominos et al. [27] showed that for methane oxidation non-uniform catalyst distributions have the potential to achieve lower thermal stresses. Khanaev et al. [29] showed that in an adiabatic reactor the optimal profile is the one that monotonically decreases along the bed length in the case of an exothermal reaction and monotonically increases in the case of an endothermic reaction.

Chapter 3: Materials and Experimental Methods

3.1. Catalyst Samples

In this study the catalyst used was a commercial DOC provided by Continental. The industrial monolithic catalyst with 14,5 cm of diameter and a length of 11 cm was cut in cylindrical "carrots" in shape of honeycombs with a diameter of 2,54 cm (1 inch) and a length of 2,6 cm.

Figure 2.1- At left Diesel Particulate Filter (DPF) and at right Diesel Exhaust Catalyst (DOC)

Being a commercial catalyst, we were expecting that it might be zone coated, i.e. the catalyst is not impregnated in the same way from the entry until the end; however that did not occur, by direct observation we noticed a uniform metal distribution on the monolithic catalyst. For this reason and unlike what happened in a previous study [9] the axial position of the catalyst in which the carrots were cut was not relevant and we chose to cut it at the entry, at the middle and at the end.

In order to follow a real mileage of such catalytic system four different aging were used in this study (Table 3.1). The aging conditions were chosen based on empirical knowledge acquired in other studies and in order to be representative of real driving cycles.

Table 2.1- Aging Conditions used in this study

Designation	Aging Conditions	
	Temperature (ºC)	Duration (h)
DOC 4h_750ºC	750	4
DOC 10h_750ºC	750	10
DOC 4h_850ºC	850	4
DOC 10h_850ºC	850	10

Figure 2.2 - Catalyst samples. From left to the right: DOC 750ºC 4h, DOC 750ºC 10h, DOC 850ºC 4h and DOC 850ºC 10h

The first aging condition “4h_750ºC” is designated by reference, which means that all the results obtained with the other aged catalysts were compared to it. The purpose of this aging was to recreate the conditions of the catalyst on a new car.

Besides this condition, tree other aging conditions were defined in order to find the “right“ aging condition to compare to the reference, in other words the condition that better recreates the performance of the catalyst on a used car. For this, we must keep in mind that a converter catalyst is designed to last the life of the car, which means that the catalytic activity should never decrease drastically in comparison with the reference, because in this case it means that we “overaged” the catalyst. Nevertheless, we must obtained significant catalytic activity differences between the aged catalyst and the reference.

3.1.1. Hydrothermal aging procedure

To simulate thermal aging of a monolithic catalyst in laboratory one of most common procedures is using hydrothermal aging employing a gas mixture composed by 90% of air and 10% water vapor.

In our case, the aging was conducted in aging bench (Figure 3.3) composed by a ROHDE oven, this dispositive can reach temperatures of 950ºC and the aging can be done on the entire monolithic catalyst or on catalyst carrots of different diameters. Within the oven is placed a conical bottom quartz reactor with an exterior diameter of 232 mm and thickness of 5 mm. A pump, positioned near to the oven, injects water on the evaporator, which is vaporized and then mixed with the air; subsequently this mixture enters on the bottom of the reactor containing the catalyst. Both the air flow and the water flow are controlled by float flowmeters. The measurement of the oven temperature is done thanks to a type K thermocouple integrated on the oven wall and the regulation is done using Eurotherm 2404/2408 PID controller.

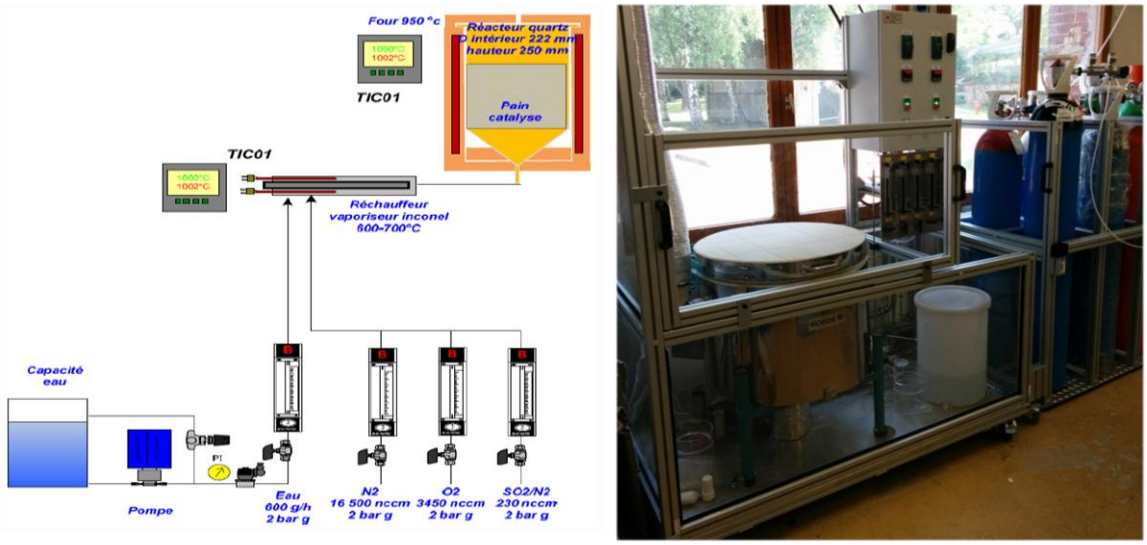

Figure 2.3- Synthetic gas bench, where the hydrothermal aging were conducted. At left schematically representation of SGB.

In the aging bench two types of aging are possible: dynamic aging (the mixture of air and water pass through the monolith catalyst) and static aging (the mixture of air and water doesn't pass through the monolith catalyst, but it creates a homogeneity mixture within the reactor). In our study, we used the second type of aging – static aging - because a previous study [9] proved that the static aging is more effective than the dynamic aging (Figure 3.4).

Figure 2.4- Representation of the static aging used in this study.

The procedure followed for preparing the "4h_750ºC" catalysts is described hereafter: four carrots of fresh catalyst were placed in the oven. Then the oven temperature and the temperature of the evaporator were increased up to 750ºC and 300ºC, respectively, at a rate of 10ºC/min, while the flow air passed through the reactor at 1150 l/h. When the oven reached 750ºC, 10% of water vapor (115 l/h) was injected on the catalyst to accelerate the aging process and the flow of air was reduced to 1035 l/h. The flows (air and water) and the temperatures (evaporator and oven) were then kept constant for four hours.

3.2. Catalytic activity studies

The catalytic activity studies were conducted in a synthetic gas bench using a synthetic gas mixture representative of the exhaust gases from diesel engines. The carrot catalyst (d=2,54 cm; L=2,6 cm) was placed inside a stainless steel reactor, which in is turn was positioned inside an oven capable of reaching temperatures up to 900ºC.

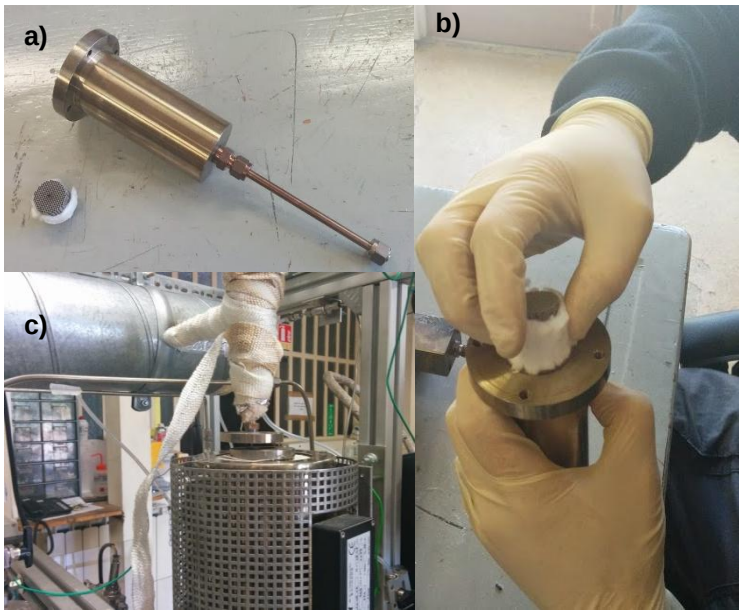

Figure 2.5- a) Stainless steel reactor and catalyst carrot b) Placement of the carrot catalyst inside the reactor c) Placement of the reactor inside the oven. Note: To force the entire gas mixture to pass through the catalyst, fiberglass insulation was used to cover the gap between the outside of the catalyst and the walls of the reactor.

To recreate real conditions, the synthetic gas bench has a serpentine heat exchanger (preheater), in which the mixture of gases is heated before entering the reactor containing the catalyst. This is done to minimize any artificial axial and radial temperature gradients during experiments.To assure a thermal homogeneity on the preheater, this device was thermally insulated using fiberglass insulation. The tubes that connected the preheater to the oven were also thermally insulated to minimize the heat loss.

The temperatures in the reactor and in the preheater were controlled by *Eurotherm 2404/2408* PID controllers. Two temperature programs were defined: one for the reactor and the second one for preheater.

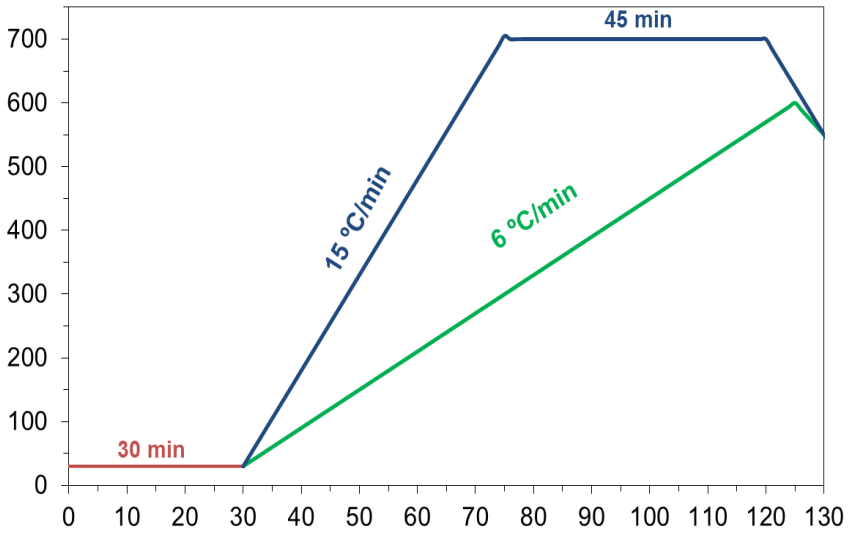

Figure 2.6- Temperature Program defined in the reactor (green) and in the preheater (blue). The red "zone" corresponds to the saturation of the catalyst.

About the temperature programs various aspects are noteworthy:

- ✓ Several adjustments had to be done in the temperature programs in order to reach an inlet catalyst temperature on the desired range (400ºC- 500ºC).
  On the first version of the programs the heating rate was defined as being the same for the reactor and for the preheater (12ºC/min), but we noticed that the increase of temperature on the preheater is slower than the increase of temperature on the reactor. This fact can be explained in two ways: the preheater was not well thermally insulated, which was not the case, or the electrical resistance was not working properly, this assumption seems more appropriate.
  For this reason, we decided to increase quickly the temperature (15ºC/min) of the preheater and then create a plateau at 700ºC with duration of 45 minutes.
- ✓ The preheater is heated at higher temperatures than the reactor in order to increase the reaction exothermicity.
- ✓ Due to the good thermal insulation of the preheater and a certain inertia on the PID controllers, the decrease of temperature on the preheater starts 5 minutes earlier

To follow the reaction temperature, two thermocouples were used, one placed at the entry of the reactor i.e. prior to the catalyst and the other positioned at the exit of the reactor. Two thermocouples were also used in the pre-heater, one at entry of the device, to measure the temperature, and the other at the exit, to control the temperature and to avoid overheating the device.

With the purpose of doing two experiments per day a cooling system was installed employing a *Lauda Ecoline RE106* refrigerating circulation chiller. In this apparatus, the air, entering at room temperature, is cooled up to -10ºC and then flows through the interior of the preheater and the reactor exterior, thus cooling both equipment's. To increase the heat exchange between the refrigerant fluid and the air, a serpentine made of stainless steel was placed inside the cooler.

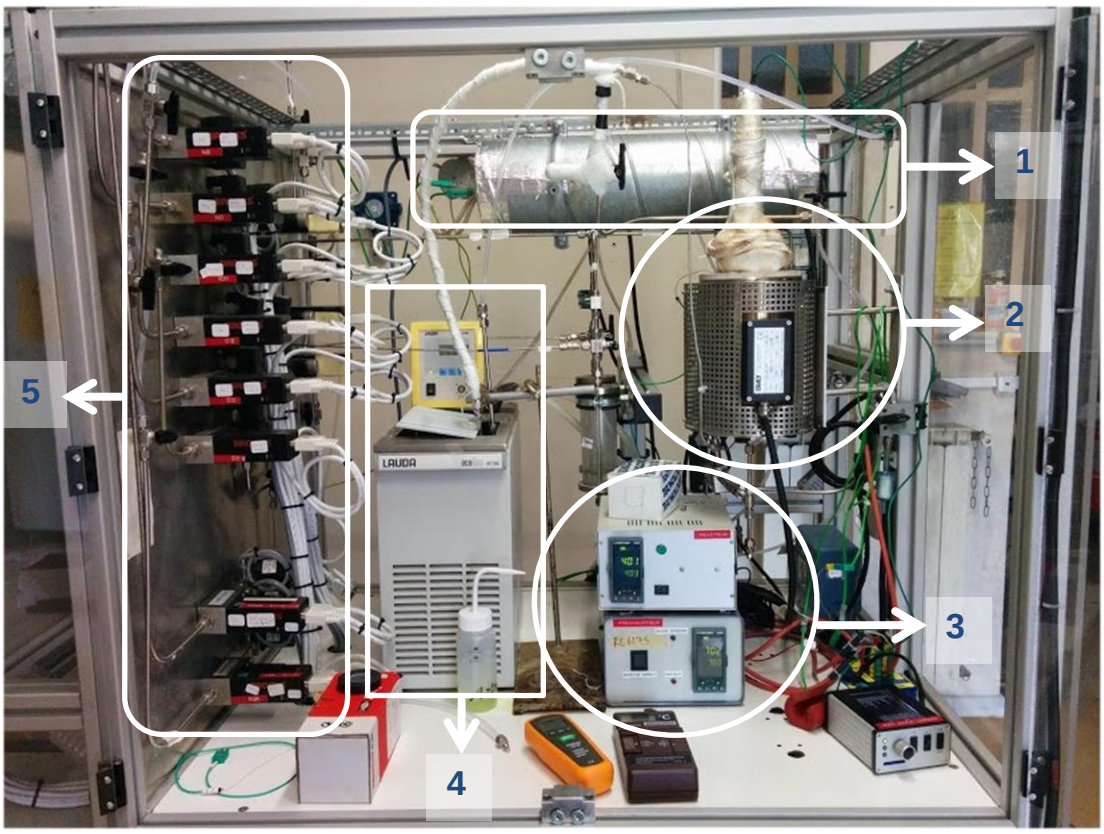

Figure 2.7- Scheme of the synthetic gas bench. 1) Serpentine heat exchanger (preheater); 2) Oven in which the reactor is placed; 3) Eurotherm 2404/2408 PID controllers; 4) Refrigerating circulation chiller 5) Volumetric flow controllers (Flowmeters)

In order to ascertain the catalytic activity of the catalyst, the reactor outflow was continuously analyzed in Environment S.A. Analyzer Bench, which is composed by several detectors:

- NOx Topaze 32 M Detector: Allowed the simultaneous detection of NO, NO_2 and NO_x ($NO+NO_2$). Its principle of detection is based on chemiluminescence, briefly described below. This detector was calibrated to detect NO_x in the range between 0-1000 ppm.

NO is a relatively unstable molecule which will oxidize to NO_2 (especially) in the presence of O_3. This reaction produces a quantity of light for each NO molecule which is reacted. This light can be measured using a photomultiplier tube or solid state device.

$$NO + O_3 \rightarrow NO_2 + O_2 + h\nu \quad \textbf{(3.1)}$$

Chemiluminescence reaction of NO to NO2

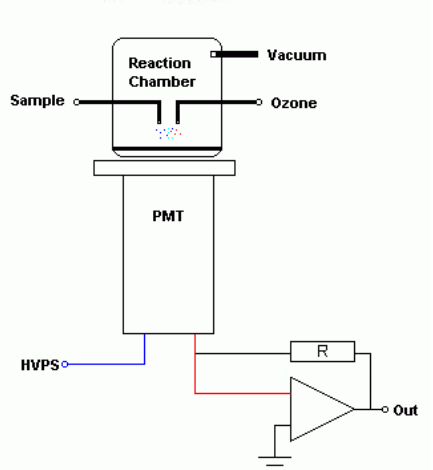

Figure 2.8- Simplified scheme of NOX detector

If the amount of ozone present is sufficient to react all of the nitric oxide, then the quantity of light produced by the reaction will be proportional to the concentration of nitric oxide in the gas sample. To measure the total oxides of nitrogen (NO_x), the sample pass over a heated catalyst to reduce all the oxides of nitrogen to NO.

- HC Graphite 52M Detector: This Flame ionization detector analyzes the total concentration of Hydrocarbons (HC). A briefly description of its detection principle its present hereafter. The chosen range was 0-1000 ppm.

In an FID the sample undergoes combustion in a hydrogen/synthetic air flame. Ions and free electrons are formed in the flame. The charged particles produce a measurable current flow in the gap between two electrodes in the detector.

The resulting current flow is of greater strength than the signal produced by the pure carrier gas and the fuel gas flame alone. This signal differential provides information about the sample. The current is proportional to the rate of ionization which in turn depends upon the concentration of HC in the sample gas.

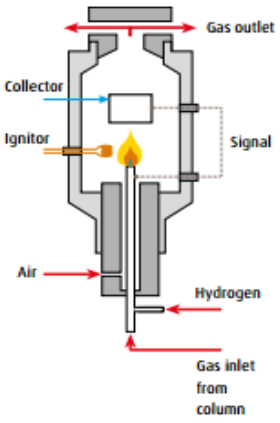

Figure 2.9 - Simplified scheme of hydrocarbons detector

- O_2/CO/CO_2 MIR 3M Detector: Allowed the simultaneous monitoring, via infrared spectroscopy of the concentration O_2, CO and CO_2. The chosen range was 0-21%V for O_2, 0-16%V for CO_2 and 0-2000 ppm for CO.
- NH_3 UV-TF Detector: Analyzes via UV NH_3 species. This detector was not used in this study.

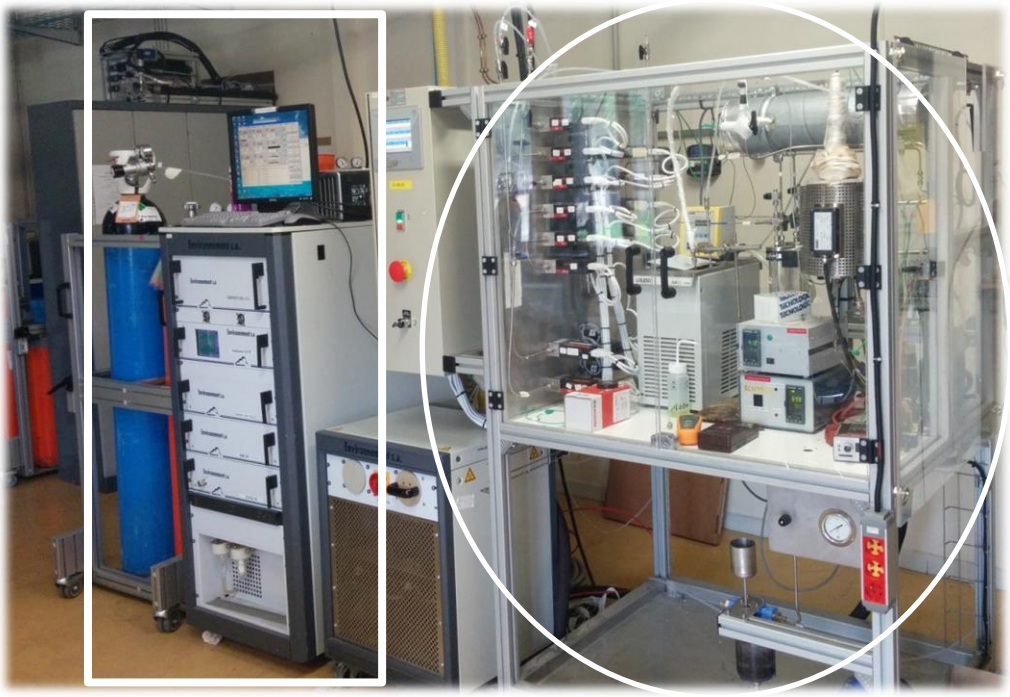

Figure 2.10- From left to the right Environment S.A. Analyzer Bench and Serv' Instrumentation Synthetic gas bench

In this study several gases (some of them mixture of gases) were used (Table 3.2). All the gases were supplied by Air liquid and the volumetric flow of each one of them was metered using calibrated volumetric flow controllers (*Brooks, Series 5850^{E}*).

Table 2.2. - Description of the gases used in this study

Gas	Composition of the gas (%V)
N_2	100% N_2
O_2	100% O_2
CO_2	100% CO_2
CO	0,25% CO and 99,75% N_2
NO	0,75% NO and 99,25% N_2
NO_2	0,80% NO_2 and 99,2% N_2
CH_4	1% CH_4 and 99% N_2

For this study CH_4 was chosen as hydrocarbon source because methane has a global warming potential of 21 (values of 2012), which means that the comparative impact of CH_4 on climate change is over 20 times greater than CO_2 over a 100-year period.

The gas hourly space velocity (GHSV) was defined as 55000 h^{-1}. Considering a cylindrical carrot with dimensions of d=2,54 cm and L=2,6 cm, the volume of catalyst (1.32×10^{-2} dm^3) was calculated, then using the equation below the total gas flow was calculated equal to 12,08 $L.min^{-1}$.

$$\mathbf{GHSV}\left(\mathbf{h^{-1}}\right) = \frac{\mathbf{Total\ gas\ flow}(\mathbf{dm^3 h^{-1}})}{\mathbf{Volume\ of\ the\ catalyst}(\mathbf{dm^3})} \quad \textbf{(3.1)}$$

Given the total gas flow, the volumetric flow of each one the gas mixture was calculated as follows:

$$\text{Volumetric Flow}_{\text{Gas x}}(\text{dm}^3\text{h}^{-1}) = \text{Total gas flow}(\text{dm}^3\text{h}^{-1}) \times \frac{\text{C}_{\text{Gas x,Desired}}\ (\text{ppm})}{\text{C}_{\text{Gas x,Bottle}} \times 10^{-2}(\text{ppm})} \quad \textbf{(3.2)}$$

In which:

$\mathbf{Volumetric\ Flow_{Gas\ x}}$ – Volumetric flow of the gas x

$\mathbf{C_{Gas\ x,Desired}}$ – Desired Concentration of the gas x. This value can be found on the table 3.3.

$\mathbf{C_{Gas\ x,Bottle}}$ – Concentration of the gas x in the bottle . This value can be found on the table 3.2.

The study consisted in temperature programmed surface reaction essays. The objective of each essay was to determine the light off curve of each pollutant (NO, CO and CH_4) present in the mixture of gases used.

The catalytic activity study was divided in two parts, whose main difference was the catalyst used: DOC reference (DOC 750ºC_4H) for the first part and DOC aged for the second part. The catalyst chosen for the second part was DOC 850ºC_4H.

The essays conducted with the DOC reference catalyst, had two goals: Firstly, using simple gas mixture (Essay 1 and 2), the purpose was to investigate the DOC performance on the oxidation of CH_4 and NO and then gradually using more complex gas mixture - until reaching the complete gas mixture, representative of the composition of the engine outlet gas - to study the impact of each gas on the catalytic activity of CH_4 and NO obtained previously , in other words estimate the interactions effects between the different gases.

In the second part of the study and by redoing the experiments done previously using the reference catalyst, but this time on aged catalyst the objectives were: studying how the aging process affects DOC performance, by comparing the results of essay 1 and 2 using DOC Reference and using DOC Aged and investigate if the aging process affects the interactions effects observed on the first part of the study.

Table 2.3- Experimental Schedule. The base feed stream consisted of 10%O_2, 5%CO_2, and appropriate reactant gases, with N_2 as the balance. Note: Due to technical problems with the water evaporator, it was not possible to use water.

Essays	CH4 (ppmV)	CO (ppmV)	NO (ppmV)	NO2 (ppmV)	CO2 (%V)	H2O (%V)	O2 (%V)	N2 (%V)
1	600	0	0	0	5	0	10	84,94
2	0	0	300	0	5	0	10	84,97
3	600	400	0	0	5	0	10	84,90
4	600	0	300	0	5	0	10	84,91
5	600	400	300	0	5	0	10	84,87

For the determination of the DOC performance on the oxidation of NO, CH_4 and CO the efficiency of oxidation (conversion) of these gases were calculated as follows.

$$\%\ \text{Conversion}\ CH_4 = \frac{X_{CH_4\ in} - X_{CH_4\ out}}{X_{CH_4\ in}} \qquad (3.3)$$

$$\%\ \mathbf{Conversion\ NO} = \frac{\mathbf{X_{NO\ in} - X_{NO\ out}}}{\mathbf{X_{NO\ in}}} \qquad (3.4)$$

$$\%\ \mathbf{Conversion\ \ CO} = \frac{\mathbf{X_{CO\ in} - X_{CO\ out}}}{\mathbf{X_{CO\ in}}} \qquad (3.5)$$

In which:

$\mathbf{X_{gas\ x\ ;\ in}}$: Inlet concentration in the catalyst of the gas x , expressed in ppmV

$\mathbf{X_{gas\ x\ ;\ out}}$: Outlet concentration in the catalyst of the gas x expressed in ppmV

3.2.1. Briefly description of the procedure followed for the characterization of the catalyst activity

1. Start recording temperatures at entry of the catalyst and temperatures and concentrations (NO, NO_x, CO, HC, CO_2, O_2) at outlet of the catalyst;
2. Cleaning the reactor and leak test;
3. Preparing the desired gas mixture in bypass (the mixture doesn't pass through the reactor);
4. Saturation of the catalyst with the gas mixture for 30 min;
5. Start increasing the temperature in the preheater and the reactor, while following the variation of the concentration of the intended gases.

When the highest temperature of the reactor it's reached, approximately 2h15 after the start of the heating program, put the mixture in bypass and do the step 2 or cool the reactor for the next essay.

3.3. Characterization of the catalyst

The characterization of the catalysts is vital; because the catalyst physicochemical composition plays an important role on the catalyst behavior, thence understand the catalyst composition may explain the results obtained in the catalytic activity essays.

As mentioned before, in this study a commercial catalyst was used, which means that available information about its composition is reduced. Besides that, and as previously discussed, the emissions regulations have become more stringent, and therefore the complexity of exhaust catalysts has increased over time, thus hindering the catalyst characterization.

For this reason, several characterization techniques were used to identify the physicochemical composition of those catalytic materials, as well as to investigate the effect of the hydrothermal aging on the surface of the catalyst. The samples for the several techniques were prepared by finely crushing the catalyst carrots and both the washcoat and support were analyzed.

Which one of the four characterization techniques are briefly described below.

- **Identification of the crystallographic phases – X-ray Diffraction (DRX)**

The X-ray Diffraction (DRX) allows the identification of the different crystallographic phases presented on each monolith catalyst. This characterization technique is based on diffraction of a monochromatic beam of X-rays by a crystalline compound.

The identification of the presented crystallographic phases on the catalyst was done using the fiches published by International Centre for Diffraction Data (ICDD). Powder XRD patterns of each catalyst were collected on a Bruker D8 Advance diffractometer equipped with a graphite monochromator and using Cu-Kα radiation. A step size of 0.02º (2θ) and a step time of 12 s were employed during acquisition. DRX measurements were conducted in CQE-IST's X-ray diffraction facility and were performed between 5º and 70º.

- **Measurement of the specific surface area- Physique adsorption of azote(BET)**

In order to understand the mechanism of aging of DOC, it's necessary to determine the textural proprieties of the catalysts before and after the hydrothermal aging, i.e. characterizing the evolution of the textural properties like specific surface. Specific surface is one of the most important textural proprieties and can be used for correlating the physique chemical proprieties of the catalyst with its reactivity.

The specific surface area of powder is determined by physical adsorption of nitrogen, on the surface of the solid and calculating the amount of the solid of adsorbate gas corresponding to a monomolecular layer on the surface applying de Brunauer, Emett and Teller (BET) method. The determination is usually carried out at the temperature of liquid nitrogen.

The adsorption and desorption isotherms of Nitrogen were measured using a Micromeritics ASAP 2010 apparatus.

Noteworthy is the fact that prior to the determination of the specific surface area of the sample, a pre-treatment by heating under vacuum $(2 \times 10^{-3} torr)$ at 200ºC for 2 hours, designed by outgassing, was done to remove gases and vapors that may have become physically adsorbed. This step it's fundamental, because if outgassing is not achieved, the specific surface may be reduce or may be variable, since part of the surface area was already covered with molecules that were previously adsorbed.

- **Precise analyses of the microstructure- Transmission Electron Microscopy(TEM)**

The transmission electron microscope uses a high energy electron beam transmitted through a very thin sample to image and analyze the microstructure of material with atomic scale resolution. Combining different modes of observation on the same catalyst sample, accurate information about the morphology, crystal structure and defects, crystal phases and composition can be obtained.

In this study TEM analysis allowed the investigation of both particle size and composition in the reference state, as well as the change induced by the different states of hydrothermal aging.

- **Determination of the number of reducible species - Temperature Programmed Reduction – TPR**

This technique determines the numbers of reducible species present in the catalyst and the temperature at which the reduction of each species occurs.

H2-TPR measurements were performed on a BELCAT-M-183 apparatus under 5%V H_2 in Argon flow. Argon is generally used as a carrier gas for hydrogen because it allows an optimization of the thermal conductivity difference between the reactant and the carrier gas. Besides that, five percent (by volume) it's the usual concentration because it provides not only a great deal of instrument sensitivity, but also a high safety factor.

The procedure followed is described hereafter: An amount between 50-60 mg of the sample was mounted in a quartz reactor that is placed in an electric furnace. Prior to the TPR, the sample undergoes a pre-treatment under flowing argon (flow rate of 50 mL min^{-1}) from room temperature to 500 ºC (5 ºC.min^{-1}), kept at 500 ºC for 1 h and then cooled to room temperature (RT). The reduction process was carried out under a mixture of 5% H_2/Argon with a flow rate of 50 mL.min^{-1}, from 60ºC to 900 ºC, at a heating rate of 7.5 ºC.min^{-1}. The H_2 mixture was stabilized in by-pass of the reactor and was put into contact with the catalyst only at the beginning of the temperature ramp.

The hydrogen consumption by the catalyst as function of temperature is derived by the change in the thermal conductivity of the gas mixture monitored by a thermal conductivity detector. The effluent gas is passed through a water trap containing a molecular-sieve trap to remove water, then through the thermal conductivity detector. Removing water is important because it is well known that water has an influence upon the signal of the detector and its presence does not allow a correct integration of the reduction peaks for the quantification of H_2 consumption.

The quantification, in moles, of H_2 consumption was determined by integrating the TPD spectrum obtained and by comparing that to the average area obtained in the loop calibration pulses.

The loop calibration pulses, consisted in the manual injection of argon into the reactor through a high precision loop valve system, in order to simulate the peaks obtained when the hydrogen is consumed. It's important to emphasize that prior to this; the signal on the TDC is stabilized under a 5%V H_2 in Argon flow. The number of moles of H_2 consumed correspondent to each peak can then be calculated as follows:

$$\left(n_{H_2}\right)_{cal} = \frac{P \times V_{loop} \times x_{H_2}}{R \times T} \qquad \textbf{(3.6)}$$

In which:

$\left(\mathbf{n_{H_2}}\right)_{\mathbf{cal}}$ – Number of moles correspondant to each peak of calibration(μmol)

$\mathbf{V_{loop}}$ – Volume of the loop valve system(m^3)

$\mathbf{x_{H_2}}$ – Volumetric percentage of H_2 in the bottle of H_2/Argon $\left(\frac{\%V}{10^2}\right)$

R – Universal Constant of Ideal Gases $(\mathrm{m^3.Pa.K^{-1}.mol^{-1}})$

T – Temperature of the gas at entering of the reactor (K)

The peaks of H_2 consumption, generally five, are then integrated and the average area is determined. This area corresponds to the number of moles of H_2 consumed calculated above.

$$\overline{A}_{cal} = \left(n_{H_2}\right)_{cal} \qquad \textbf{(3.7)}$$

A relation between the moles of H_2 consumed and the area of the peaks can be then established (Equation).

$$n_{H_2,P_x} = \left(n_{H_2}\right)_{cal} \times \frac{A_{P_x}}{\overline{A}_{cal}} \qquad \textbf{(3.8)}$$

In which:

$\mathbf{n_{H_2,P_x}}$ – Number of moles correspondant to a H_2 consumption peak (µmol)

$\mathbf{A_{P_x}}$ – Area of the H_2 consumption peak ($\frac{\mu V}{s}$)

$\mathbf{\overline{A}_{cal}}$ – Average area of the calibration peaks ($\frac{\mu V}{s}$)

To normalize the values of n_{H_2,P_x} are divided for the mass of the sample.

Chapter 4: Results and Discussion

This chapter is divided in two main sections. In the first section the obtained results for the different characterization techniques performed on the different diesel oxidation catalysts are presented. This section comprises the analysis of the textural and morphological proprieties by BET and TEM measurements, the determination of the number of reducible species present in the catalyst by TPR and finally the characterization of the presented crystallographic phases by DRX.

In the second section the correlation between the evolution of the catalyst surface morphology and its catalytic performance, namely in the oxidation of hydrocarbons and NO, after the aging is presented. Furthermore the estimation of the interactions effects between the different gases is shown.

4.1. Characterization of the catalyst

4.1.1. Brunauer, Emett and Teller (BET) analysis

Table 4.1 shows the textural parameters for the reference catalyst and aged catalysts. It can be seen that the textural properties for the two first aging (750ºC_10h and 850ºC_4h) are similar to those measured for the reference catalyst (750ºC_4h), suggesting that those aging conditions had nearly no influence on the surface state of the catalyst. Unlike what was expected the surface area and total pore volume for 850ºC_10h catalyst increased, comparatively to the reference catalyst. We were expecting, the formation of bigger pores and the decrease of specific surface¸ due to metal sintering during the aging process.

This result indicates that this aging condition, actually activate the catalyst surface; perhaps due to the unblocking of pores or due to a phase transformation in the support. Further analysis, would be necessary to detected if there are changes in the support structures of the catalyst. It's important to emphasize that the surface area measured take into account the specific surface of cordierite, however this surface can be neglected (more or less 1 m^2/g).

Table 4.1 -Textural parameters for the reference and aged catalysts.

Sample	Surface area (m^2/g)	Total pore volume (cm^3/g)	Mean pore diameter (nm)
750ºC_4h	53	0,13	9,69
750ºC_10h	52	0,13	9,95
850ºC_4h	51	0,13	10,08
850ºC_10h	83	0,19	9,22

4.1.2. TEM analysis (Transmission Electronic Microscopy)

The results of the analysis of the reference catalyst (750ºC_4h) surface by TEM are shown in figure 4.1; in the center is shown a picture of the reference catalyst and in the upper right corner a EDS(Energy Dispersive spectroscopy) analysis performed on the zone marked with a white circle.

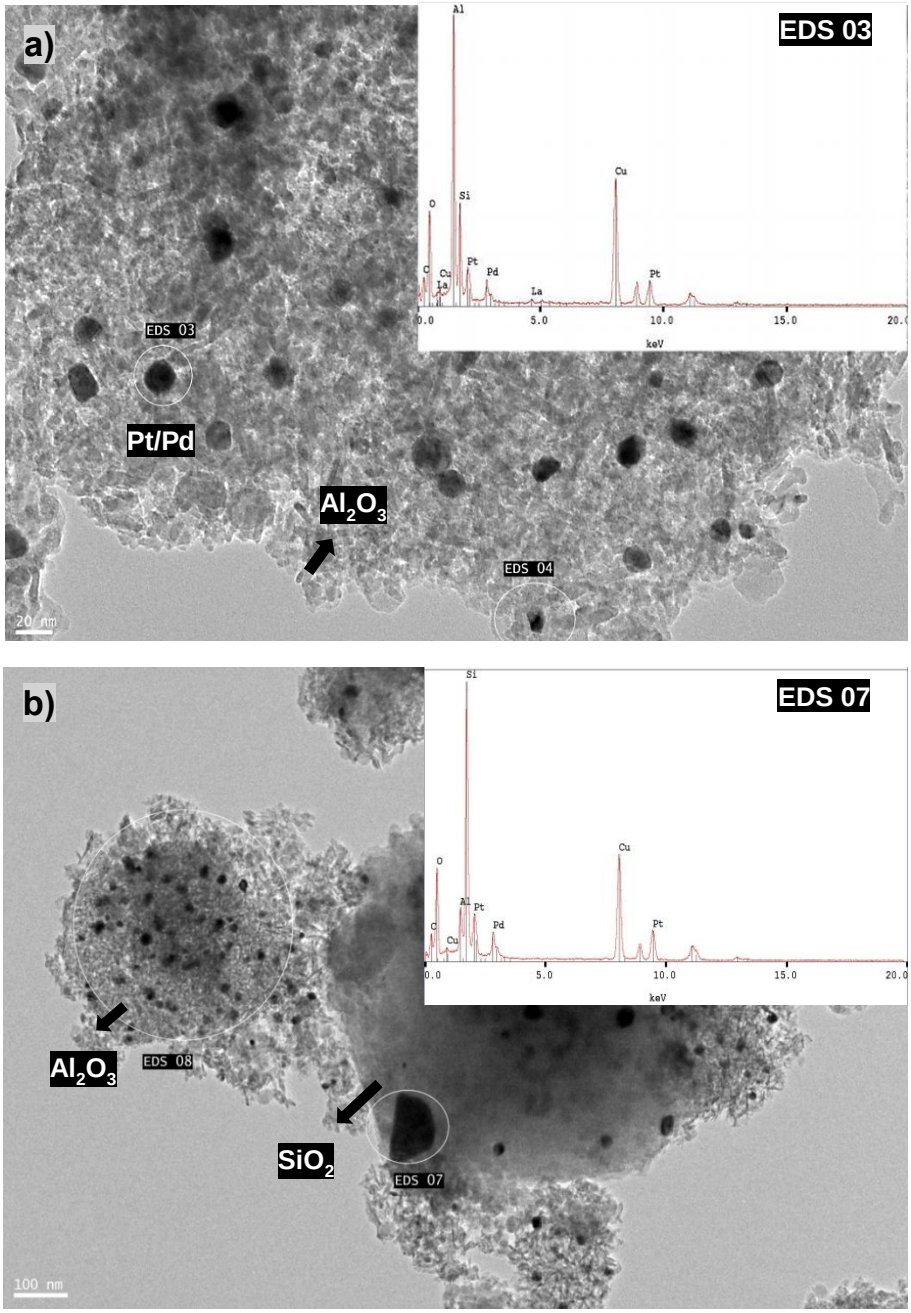

Figure 4.1- TEM images of the reference catalyst (750ºC_4h) and at upper right corner an EDS analysis of the zone marked with a white circle.

From figure 4.1 one can conclude that the support is predominately composed by aluminum and silicon. These two elements are presented in the form of oxides: alumina (Al_2O_3), which is the main washcoat material and silica (SiO_2). Traces of lanthanum was also found, this element in the form of an oxide (La_2O_3) is commonly used as a support additive to improved thermal stability of the support. Silica is also used as a support additive for alumina. Globally was verified that the affinity of the metal particles for the alumina support is greater than their affinity for the aluminosilicate support.

Regarding the active components, TEM analysis indicates that the noble metals presented are palladium and platinum, most likely in bimetallic complex because they appear simultaneously in all the EDS analysis. Platinum is presented in a large amount, however to know the exact Pt/Pd proportion an elementary analysis by X-ray fluorescence would be necessary. This analysis would also provide information concerning the evolution of the noble metals content with the aging, and if a decrease of this parameter was observed i.e. loss of active phase, one could conclude that a portion of the precious metal species was entrapped. To ascertain the oxidation state of metal particles X-ray photoelectron spectroscopy (XPS) would also be necessary. Cooper was also encountered; its presence was also reported on a previous DOC study [9]. Additionally a pore distribution study would also be very important, to completely understand the aging phenomena.
The chemical composition of the catalysts exposed to hydrothermal aging was identical to the reference catalyst, excluding DOC 850ºC_10h, where the presence of other support elements (manganese, titanium, magnesium, rhodium and nickel) were detected.

The effect of aging on the surface state of the different catalysts was followed by TEM, providing information about the distribution and size of the metal particles on the catalyst surface (figures 4.2 and 4.3).

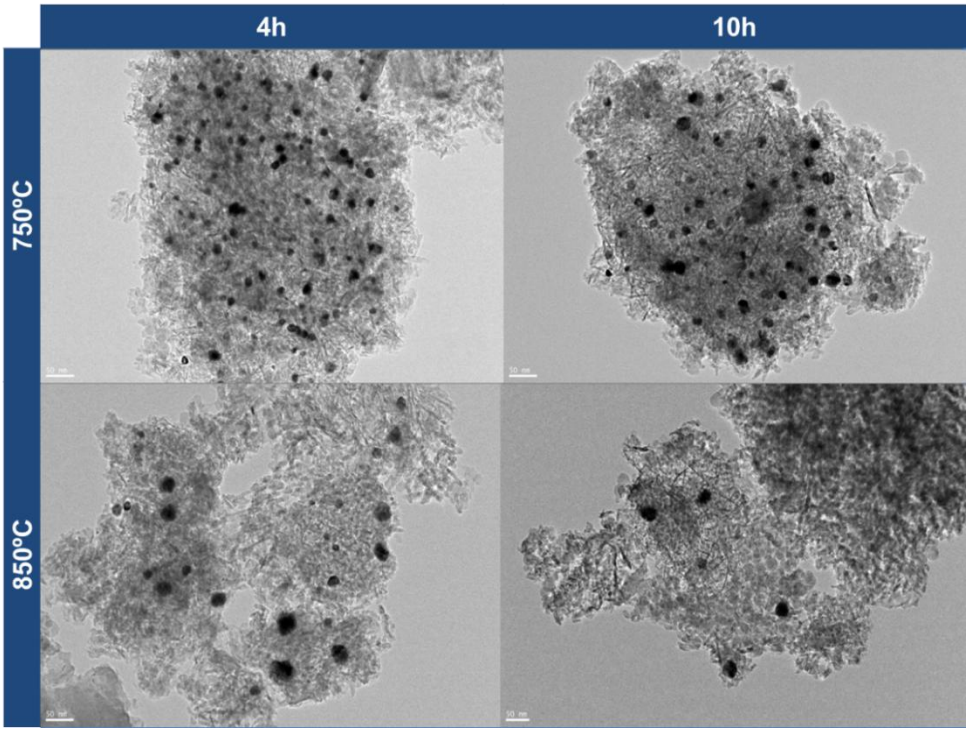

Figure 4.2- TEM images for reference and aged catalysts. Influence of aging on the surface of the catalyst.

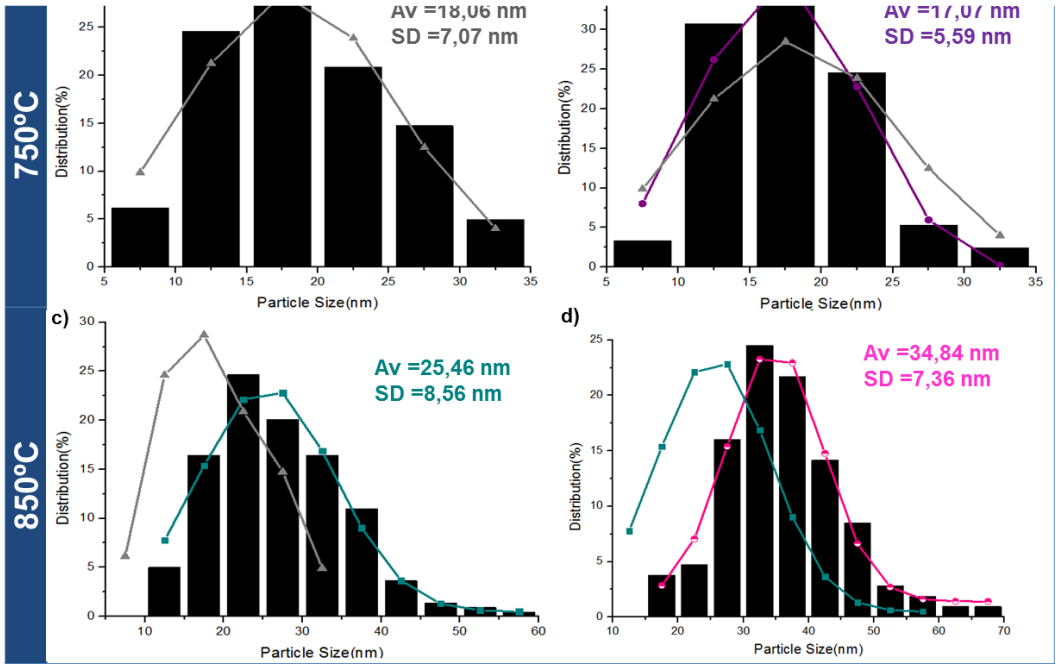

Figure 4.3- Evolution of the particle size distribution with the aging. Av: Average SD: Standard Deviation.

In the figure 4.2a and figure 4.3a one can see that for the reference catalyst (750ºC_4h) the particle distribution on the catalyst surface is rich and homogeneous, with particles between 5-35 nm. The histogram of the figure 4.3a indicates that the majority of the particles had a size between 10-25 nm. These results provide us information about the particle reparation on the reference catalyst, allowing the study of aging impact on this particle distribution.

Comparing these results, with those obtained for 750ºC_10h, we can observe that the particle size remained in the same rage, but the particles between 10-20 nm increase their proportion, which is partly explain by the agglomeration of the particles with the size between 5-10 nm. We also noticed that the proportion of larger particles decreased, which might be explained due to the redispersion of particles. Nevertheless, globally we didn't observe significantly differences in the particle reparation between the reference catalyst and the 750ºC_10h catalyst (figures 4.2b and 4.3b). For the 850ºC_4h catalyst (figure 4.3c), the particles size was majority comprised between 20-35 nm and particles between 35-60 nm, nonexistent on the reference catalyst were also found. Furthermore, the minimum particle size increased to 10 nm. These results are explained by the diffusion of the small particles to form other particles with a larger size, a phenomenon, previously described, called sintering.

Finally, figure 4.3d shows that for 850ºC_10h catalyst the particle distribution continued to increase, being that the particle size rage was between 15-70 nm, with the majority of the particle population between 25-40 nm.

The observed sintering has significant effects on the performance of the catalyst; this effect will be investigated on the next section, with especial effect on the surface reaction velocity, due to the decrease on the available active surface for the oxidation reactions.

After the sintering, the contact surface between the noble metals and the pollutant gases is significantly decreased, thus decreasing the catalytic activity of the catalyst. It's important to emphasize that this phenomenon is irreversible and it has an impact on the performance of the catalyst during its entire lifetime.

4.1.3. DRX analysis (X-ray Diffraction)

The X-ray diffraction analysis allows revealing the different crystallographic phases presented in the reference catalyst and aged catalysts.

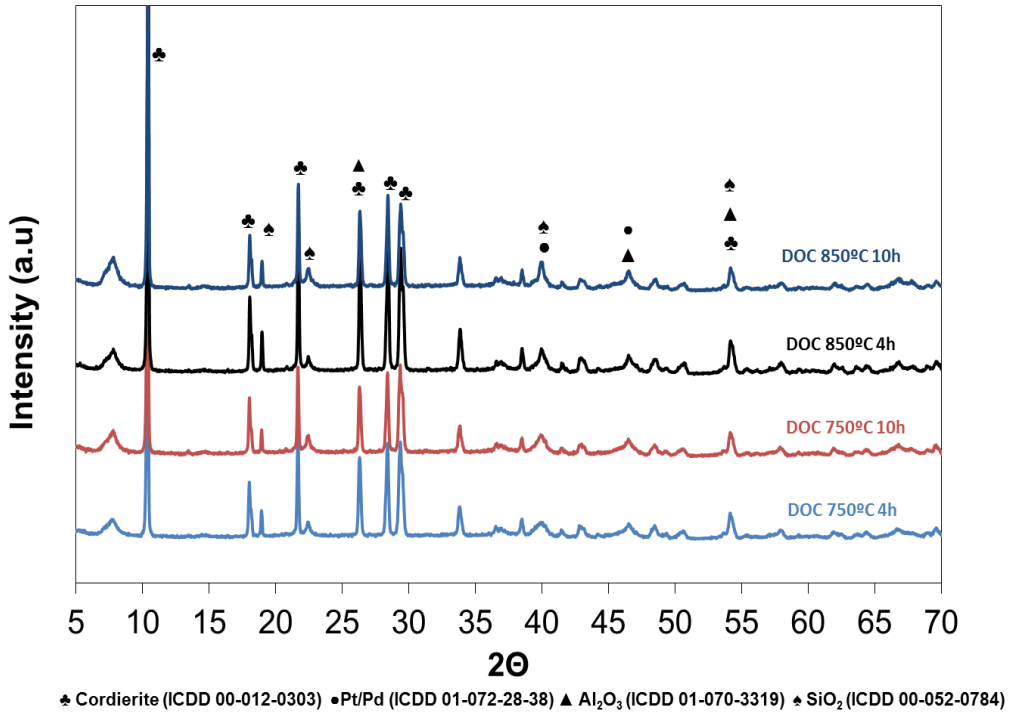

Figure 4.4-X-ray diffractograms of the reference catalyst and aged catalysts.

From the observation of figure 4.4 one can confirm the presence of alumina (Al_2O_3) and silica (SiO_2) as support and as active phase a bimetallic complex of Pt/Pd. Cordierite was also found, what was expected because DOC is based on cordierite "honeycomb" monoliths. It was not possible to confirm the presence of La_2O_3.

Comparing the different X-ray diffractograms it's seen that they are similar, i.e there was no appearance of a new peak or shift of an existing peak, the only noticeable change is the increase in the intensity of the peak correspondent to 2Θ=40 (Pt/Pd), corroborating the agglomeration of metal particles (metal sintering) previously seen in TEM results.

4.1.4. TPR analysis (Temperature programmed reduction)

Figure 4.5 displays H_2-TPR profiles for the reference (750ºC_4h) and aged catalysts. Excluding the 850ºC_10h catalyst, the remained catalysts feature a single broad peak at about 644,9-783,4ºC, which are most likely attributed to the reduction of the support composed by alumina and silica, due to high temperature in which it occurs.

It's noticeable that the peak area and therefore hydrogen consumption decreased with the aging, for the two first aging, suggesting that there was a reduction in the reduced species. This might indicate that the support structure was sintered. Nevertheless we must take into account that the DRX results do not indicate any change in the support structure.

For the 850ºC_10h catalyst one can observe an increase in the area of peak 1 and the appearance of a second peak at lower temperatures (501,5- 610ºC). These results seem to be related with the increase of surface area observed in BET analysis. An increase in H_2 consumption means that more species are available for reduction reaction and the appearance of a new peak suggests that the support suffered a phase transformation. As said earlier, further analysis would be necessary to comprehend these results.

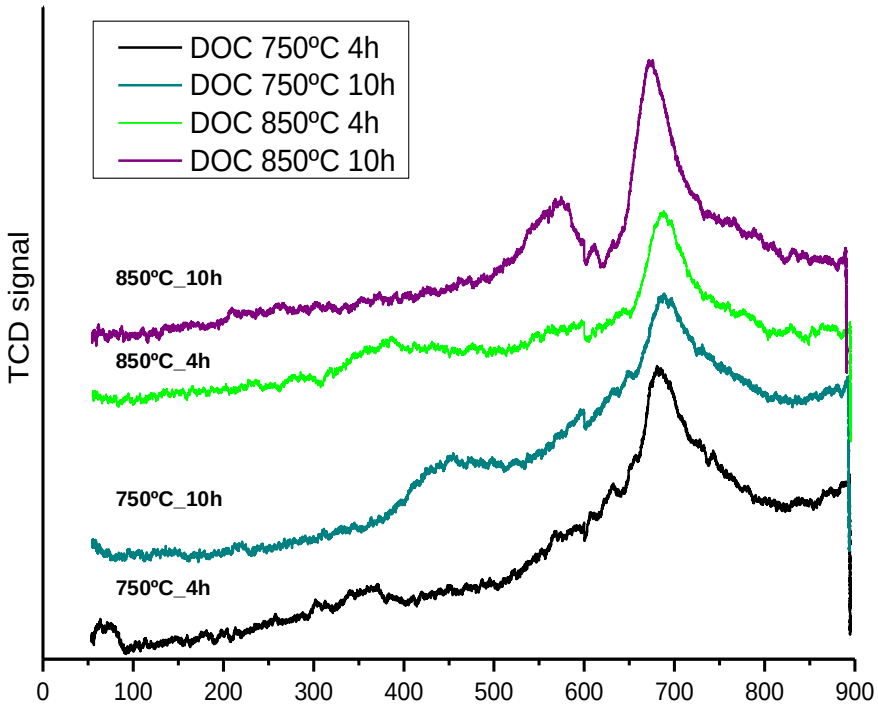

Figure 4.5- H_2-TPR profiles for the reference catalyst and aged catalysts.

Table 4.2 - TPR results: temperature and hydrogen consumption of the existent peaks for the reference and aged catalysts.

	Peak 1		Peak 2	
Sample	ΔT (ºC)	H_2 Consumption (µmol/g)	ΔT (ºC)	H_2 Consumption (µmol/g)
750ºC_4h	644,9- 783,4	4,34		
750ºC_ 10h	644,9- 783,5	3,24		
850ºC_ 4h	644,9- 783,6	3,17		
850ºC_10h	644,9- 783,7	6,51	501,5- 610	2,74

4.2. Catalytic activity essays

4.2.1. DOC performance on NO/CH_4 oxidation

The performance of the reference catalyst (750ºC_4h) on the oxidation of CH_4 and NO under lean conditions are presented in figures 4.7 and 4.8, respectively. Methane oxidation conversion was measurable at approximately 350ºC and reached a maximum of about 16% at the maximum temperature attained (393ºC), what suggests that higher conversions might have been attained if the temperature ramp was continued to higher temperatures (Figure 4.7). The lower methane conversions obtained and the high light-off temperature were expected because short carbon chain hydrocarbons are more difficult to convert in the catalyst [30]. In the data shown below, the x-axis temperature is the inlet temperature, thereby avoiding complications from exothermic generated heat on or in the sample.

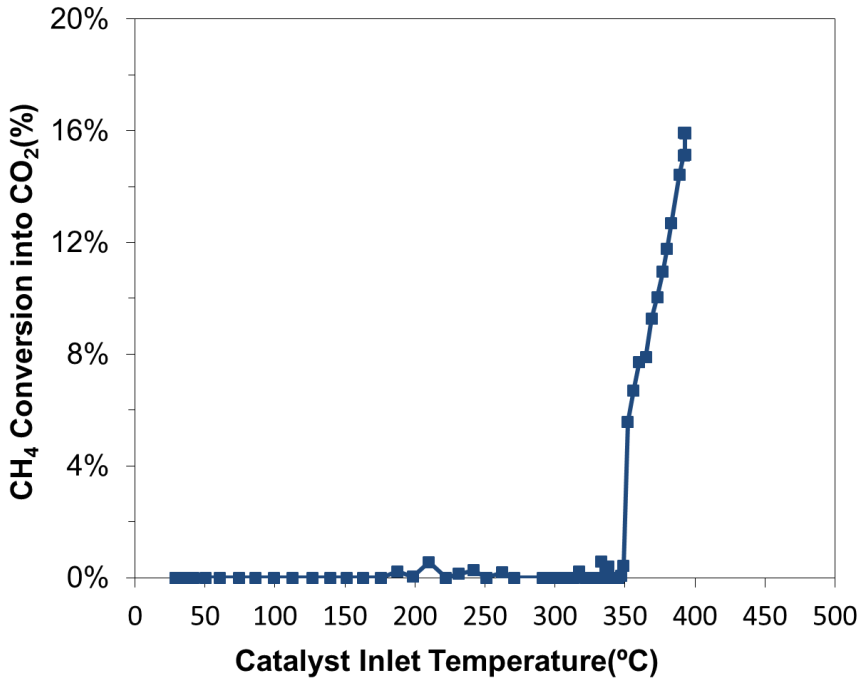

Figure 4.6- Essay 1: Methane conversion as function of the catalyst inlet temperature. The feed stream contained 600 ppmV CH_4, 5%V CO_2, 10%V O_2 and N_2 as balance. Results obtained using the reference catalyst (750ºC_4h).

NO oxidation conversion was measurable around 190ºC, and then it increases continuously with the temperature until approximately 42%, where it reaches the maximum conversion at 42%. Thereafter the NO conversion decreases, being that, at highest temperature attained (426ºC) the conversion had dropped to 40% (Figure 4.8).

This behavior was expected since, as mentioned, NO oxidation to NO_2 is limited by kinetics at lower temperatures and by thermodynamics at higher temperatures (reference). Mulla et all. [31] proposed a mechanism for this reaction, in which the rate for NO and O_2 is approximately first order, but there is an approximately negative first order dependency for NO_2.

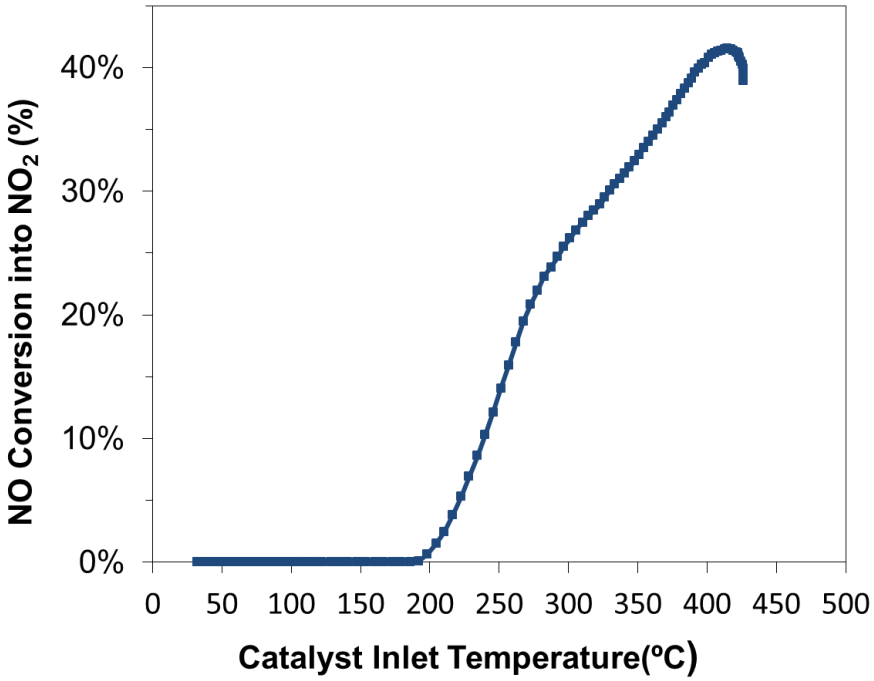

Figure 4.7 – Essay 2: NO conversion as function of the catalyst inlet temperature. The feed stream contained 300 ppmV NO, 5%V CO_2, 10%V O_2 and N_2 as balance. Results obtained using the reference catalyst (750ºC_4h).

This product inhibition imposes significant constraints on NO conversion until thermodynamic limitations are reached, typically above 350ºC [24]. In our case, NO/NO_2 equilibrium limitations were observed above 400ºC.

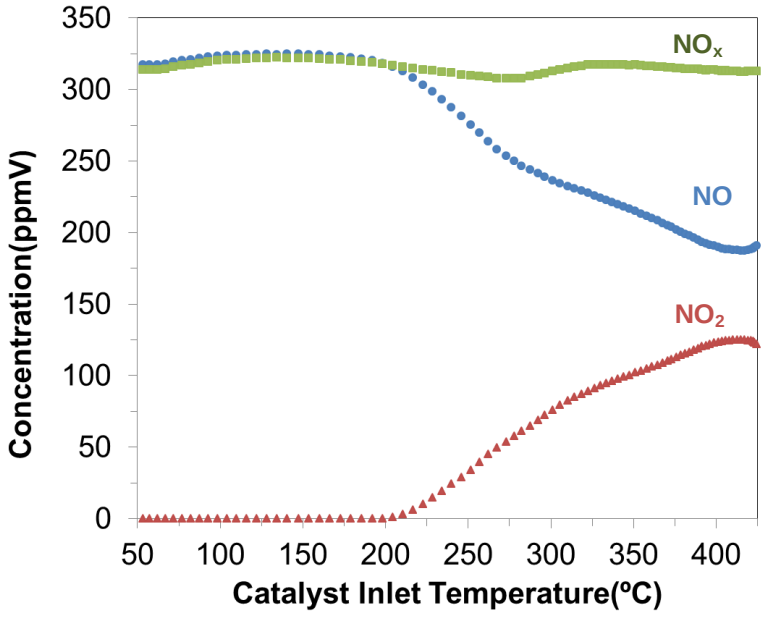

Figure 4.8 – Essay 2: Concentration of NO, NO_2 and NOx (NO+NO_2) as function of catalyst inlet temperature. The feed stream contained 300 ppmV NO, 5%V CO_2, 10%V O_2 and N_2 as balance. Results obtained using the reference catalyst (750ºC_4h).

4.2.2. Effect of CO/CH_4/NO on CH_4/CO/NO oxidation over DOC

As previously mentioned, the purpose of this section is to evaluate the effects of NO and CO on CH_4 oxidation and CH_4 and CO on NO oxidation. The light-off curves obtained from essay 1 to essay 5 are presented on figure 4.10 and figure 4.12.

The CH_4 conversions in the presence of CO are plotted in the figure 4.10b), curve named CH_4+NO. It is seen that despite the lower light off temperature (325ºC) the conversion of CH_4 across the temperature range between 350ºC and 395ºC is significantly lower, compared to data obtained for CH_4 alone, which indicates that the presence of CO has an inhibition effect on CH_4 oxidation.

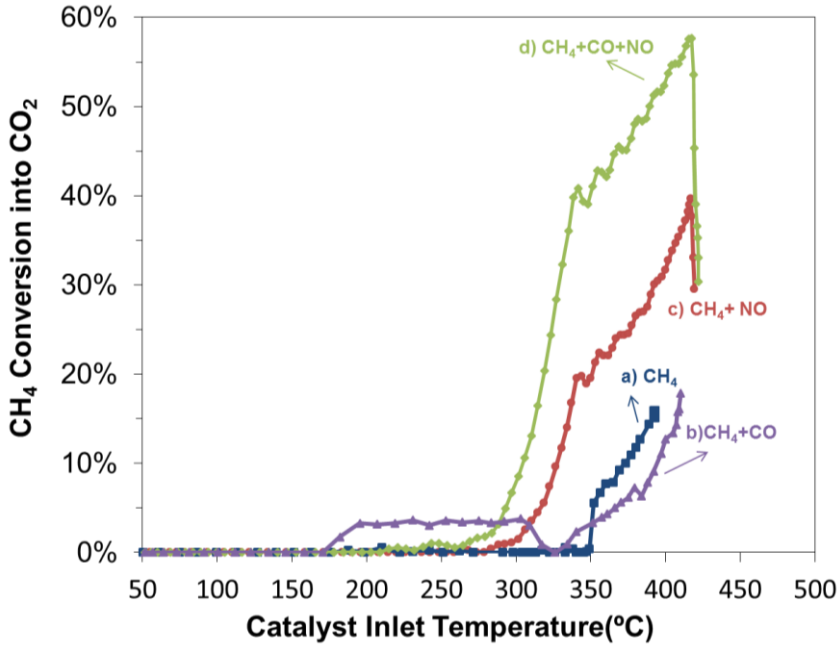

Figure 4.9- Methane conversion into CO_2 in function of the temperature: a) Essay 1: CH_4 (■) b) Essay 3: CH_4+CO (▲) c) Essay 4: CH_4+NO (●) d) Essay 5: CH_4+CO+NO (♦). Results obtained using the reference catalyst (750ºC_4h)

Furthermore, from figure 4.11, one can see that CH_4 oxidation only began after the concentration of CO became practically invariable (indicator of the maximum conversion of CO), thus confirming the CO inhibition effect on CH_4 oxidation. This inhibition effect is most likely explained by the competition between CO and CH_4 for Pt/Pd sites and since CO conversion in the catalyst it's simpler than the CH_4 conversion, the oxidation reaction rate of CO is higher than the oxidation rate for CH_4. Comparing the light-off curves, we can see that while for CO(in the presence of CH_4) the light off temperature was 146ºC, for CH_4 (alone) it was nearly 200ºC higher(350ºC).

It is noteworthy that, although we haven't done an essay where we studied only the oxidation of CO, we are almost certain that the results wouldn't be significantly different from those obtained for $CO+CH_4$.

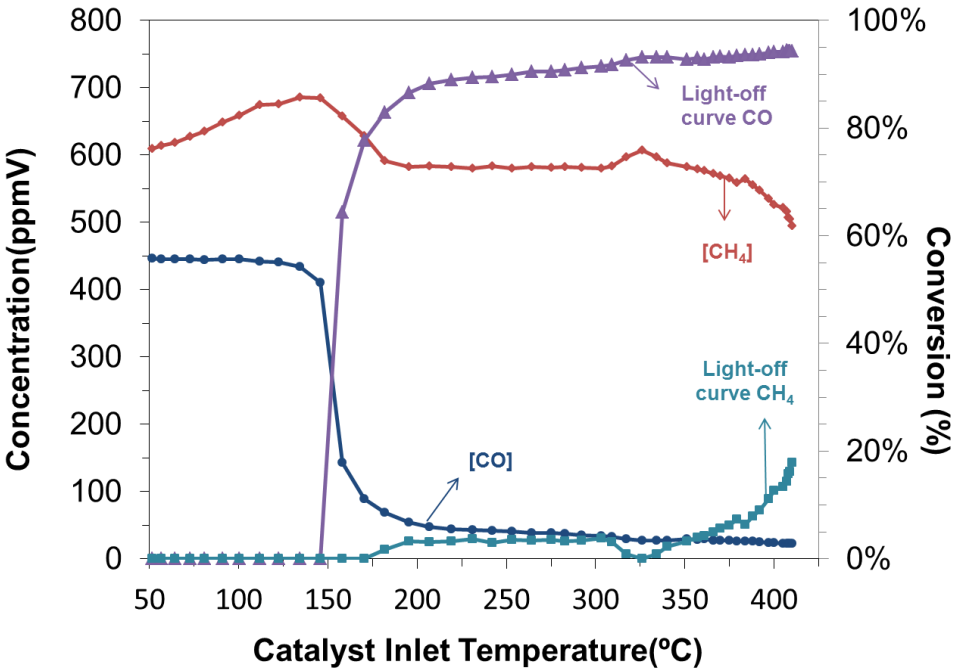

Figure 4.10- Essay 2: CO concentration (●); CH_4 concentration (♦); Light-off curve of methane (■); Light-off curve of CO (▲). Results obtained using the reference catalyst (750ºC_4h).

The effect of NO in CH_4 is shown in figure 4.10c) namely in the curve CH_4+NO. The data show that the addition of NO resulted in a significant increase in the measured CH_4 conversions to CO_2.

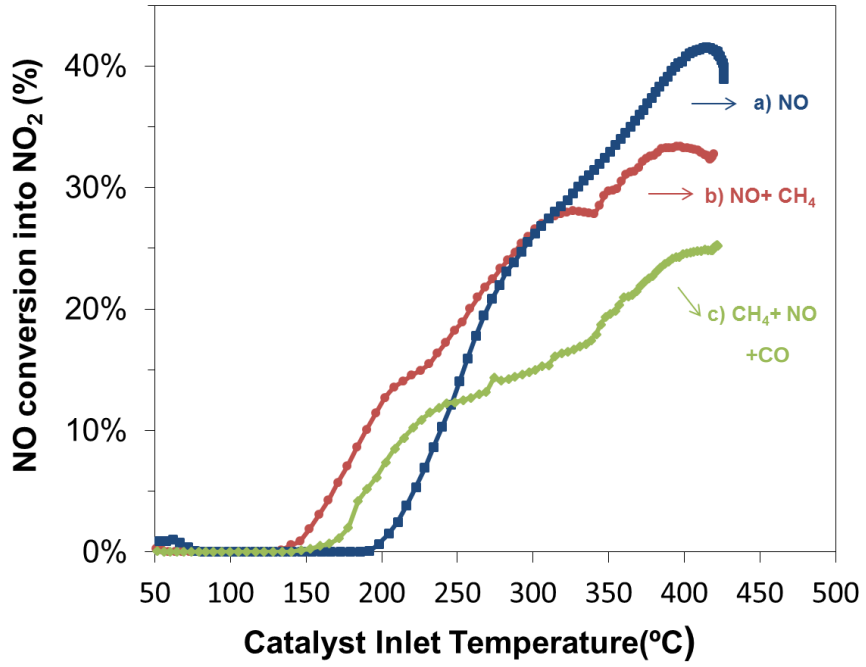

Figure 4.11- NO conversion into NO_2 in function of the temperature: a) Essay 2: NO(■);b) Essay 4: NO+CH_4 (●); c) Essay 5: CH_4+NO+CO (♦) Results obtained using the reference catalyst (750ºC_4h).

The temperature for 16% of conversion of CH_4 in Essay 4 decreased 58ºC in comparison with the same in Essay 1, and a maximum conversion of 40% at 416-417ºC was observed. Furthermore it caused the methane light-off curve to shift to lower temperatures (287-292ºC).

In parallel the effect of CH_4 in NO oxidation is shown in figure 4.12b). One can see, that although the addition of CH_4 accelerates the NO oxidation reaction (the light-off occurs 59ºC earlier), compared to NO alone, after 300ºC the light-off curve for NO in the presence of methane was below the curve with NO alone, meaning that CH_4 is inhibiting NO oxidation.

The explanation for both behaviors may be that NO_2, a product of NO oxidation, is being consumed as an oxidant in CH_4 oxidation reaction, resulting in the appearance of NO oxidation inhibition and hence in an increase of CH_4 conversions. A proposed reaction mechanism for this essay is presented hereafter:

$$CH_4 + 2O_2 \rightarrow CO_2 + 2H_2O \quad (4.1)$$

$$2NO + O_2 \xrightleftharpoons{} 2NO_2 \quad (4.2)$$

$$CH_4 + 2NO_2 \rightarrow CO_2 + N_2 + 2H_2O \quad (4.3)$$

$$Globally: CH_4 + 2NO + O_2 \rightarrow CO_2 + N_2 + 2H_2O \quad (4.4)$$

Reaction 4.4. is called selective catalytic reduction (SCR). The SCR of NO by hydrocarbons has been extensively reported in the literature over a variety of catalysts since the reaction was first reported in 1990 In addition, the partial reduction of some NO to N_2O may also occur, which is an undesirable reaction because N_2O is a strong greenhouse gas, and also leads to formation of NO in the upper atmosphere [29].

$$CH_4 + 2NO + \frac{3}{2}O_2 \rightarrow CO_2 + N_2O + 2H_2O \quad (4.5)$$

We can also potentially have the reaction between NO_2 and methane to form NO:

$$CH_4 + NO_2 + \frac{3}{2}O_2 \rightarrow NO + 2H_2O + CO_2 \quad (4.6)$$

In a study [24] concerning the effect of HC species on NO oxidation over DOC, investigators evaluated the efficiency of NO_2 as an oxidant relative to O_2 and concluded that even with high levels of O_2, almost all of NO_2 was consumed in detriment to O_2; in other words, NO_2 was being consumed preferentially in relation to the O_2.

The relation between NO_2 reduction and CH_4 oxidation is especially evident in figure 4.13. The temperature range in which the NO_2 measured in Essay 4 ($NO+CH_4$) became lower than the amount of NO_2 measured in Essay 2 (NO), meaning a consumption of NO_2, corresponds to the temperature range in which the light-off for methane occurred.

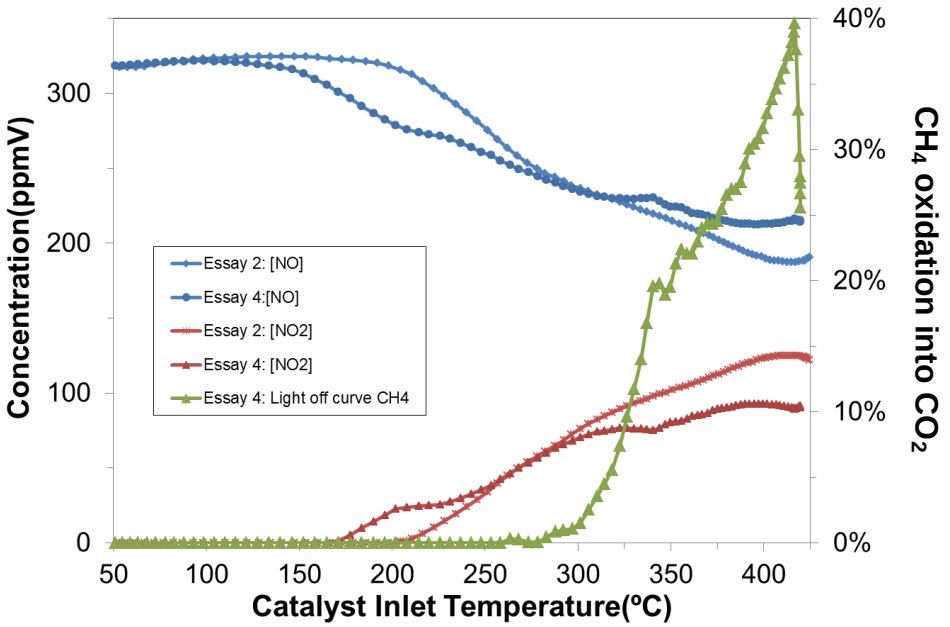

Figure 4.12- Essay 2: Concentration of NO and NO_2 in function of the temperature. Essay 4: Concentration of NO and NO_2 in function of the temperature and light-off curve methane. Results obtained using the reference catalyst (750ºC_4h).

From detailed observation of the CH_4 light-off curve for essay 4 (figure 4.10c), one can distinguish two regions in the temperature range between 283ºC and 417ºC: one that starts at the light-off temperature (283ºC) and goes until the curve inflection (344ºC) and a second section starting at that point and going until the temperature corresponding at the maximum conversion (417ºC).

There was a noticeable change in slope between the two regions: in the first region the slope was steeper than in the second one, in other words the CH_4 oxidation improvement effect diminished as the temperature increased. This might be explained due to a switch between NO_2 and O_2 as an oxidant, i.e. increase of methane reaction with O_2, which is in significantly higher amounts. This also suggests that the curve inflection marks the temperature in which the switch occurred.

In Figure 4.10d) the combined effect of CO and NO on CH_4 oxidation is also presented. Comparing the CH_4 oxidation in the presence of NO and CO (essay 5) with the same, but only in the presence of NO (essay 4), it's perceptible that while the behavior of the both light-off curves was nearly identical, being that even the curve inflection and the maximum conversion occurred in the same temperature range, the slope between the light-off and the curve inflection was more pronounced for the ignition curve in the presence of CO and NO, resulting thus in an improvement in methane oxidation.
The maximum methane conversion was 57%, compared with 40% obtained in the essay 4: CH_4+NO. Furthermore the methane light-off curve for essay 5 was shifted to the left, relatively to essay 4: CH_4+NO.

Given that, as previously discussed, CO has an inhibition effect on methane, the improvement in CH_4 oxidation in the presence of NO and CO it's most likely explained due to the effect of CO on NO oxidation, which might be somehow related to the slope increase of the region between light-off and the curve inflection and as mentioned before with the switch between oxidants.

On the contrary, the combined effect of CH_4 and CO led to a further decrease in NO oxidation (figure 4.12c), relatively to what was seen in the essay 4: CH_4+NO. Moreover, the addition of CH_4 and CO caused NO light-off to occur at higher temperature. The reason for this behavior it's not clear, and further essays would be necessary to fully understand it, namely an essay to study the effect of CO in NO oxidation and essays to evaluate the efficiency of CO_2 as an oxidant relatively to oxygen, to validate the reaction mechanism proposed below.

$$CO + \frac{1}{2}O_2 \rightarrow CO_2 \quad (4.7)$$

$$CO_2 + NO \rightarrow NO_2 + CO \quad (4.8)$$

$$CH_4 + 2NO_2 \rightarrow CO_2 + N_2 + 2H_2O \quad (4.9)$$

$$Globally: CH_4 + \frac{1}{2}O_2 + NO + NO_2 \rightarrow CO_2 + N_2 + 2H_2O \quad (4.10)$$

Moreover, from the obtained results, one can also concluded that NO has an slightly inhibition effect on CO oxidation, given that the addition of CO and CH_4 caused a delay in CO oxidation light-off, resulting in less conversion across the entire temperature range, in comparison with the essay CH_4+CO. Nevertheless, it's important to emphasize that the differences in light-off temperature(less than 10ºC) and maximum conversion(less than 3%) between the two essays are negligible.

4.2.3. Effect of aging on CH_4/NO/CO oxidation over DOC

Figures 4.14 and 4.15 show the influence of aging on DOC performance on the oxidation of NO and CH_4 for essay 1, essay 2 and essay 5. It was chosen not to show the results for all the essays, because the aging effect is similar to those presented hereafter.

For methane, the results for essay 5 show a shift on the light-off curve towards higher temperatures(approximately 40ºC) , however this had little impact on the methane conversions obtained; we obtained the same conversions but at higher temperatures. Furthermore the gap between both curves remained stable. For essay 1, despite the fact that the light-off for the aged catalyst occurred sooner (20ºC sooner), the catalytic performance of the reference catalyst was superior to the aged catalyst. These results were expected, nevertheless the decrease of the catalytic activity was not significant, which means, that the catalyst has excellent age resistance. Therefore, more drastic aging conditions (i.e. using the 850ºC_10h catalyst) would be necessary to observe a significant change in the catalyst performance after hydrothermal aging.

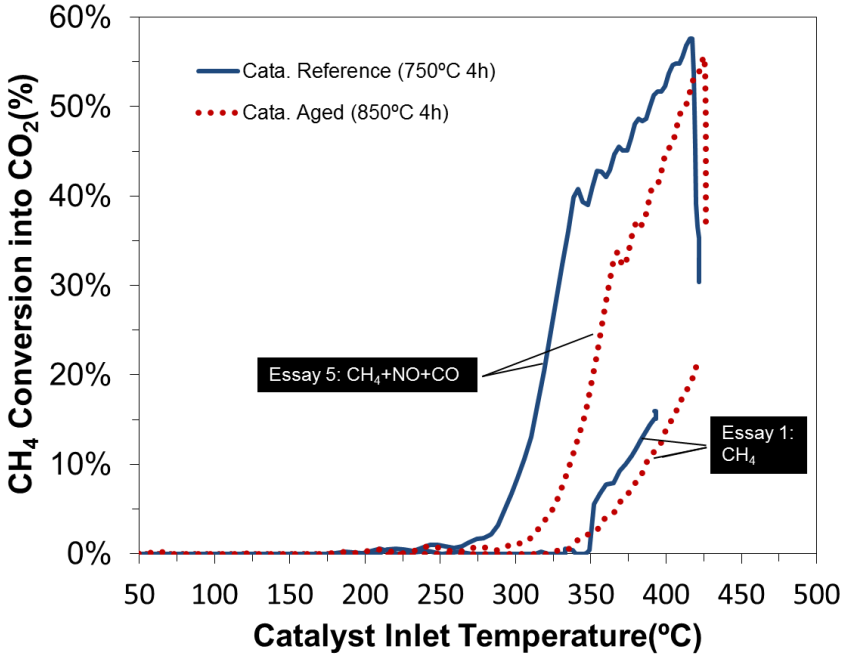

Figure 4.13-Comparison of the methane light-off curves obtained using the reference catalyst (750ºC_4h) and the aged catalyst (850ºC_4h) for essay 1 and essay 5.

On the contrary, the aging improved the NO oxidation reaction until 364ºC; comparatively to the reference catalyst, but after this temperature the light-off curve for the aged catalyst remained below the light-off curve for the reference catalyst. Furthermore, the light-off temperature for the aged catalyst was 70ºC lower than for the reference catalyst and superior conversions were obtained with the aged catalyst until 364ºC.

The improvement of the NO oxidation performance with the aging was also reported in a previous study where the authors explained that activity of the catalyst for NO oxidation depends on the size of the Pt particle, where NO oxidation is better with larger particle size. Additionally the authors reported that this has been observed with Pt supported on Al_2O_3, SiO_2, and TiO_2, and suggests that some amount of thermal aging may actually improve NO oxidation performance [24]. For essay 5 similar results were obtained with the exception of the light-off temperature that occurred in the same temperature range for the reference and the aged catalyst. For CO, the light-off occurred in the same temperature range for both catalysts, however a decrease between 10-20% in the conversion was observed in the aged catalyst, relatively to the reference catalyst.

Additionally the aging had no effect on the interactions between the different species observed in the section 4.2.2.

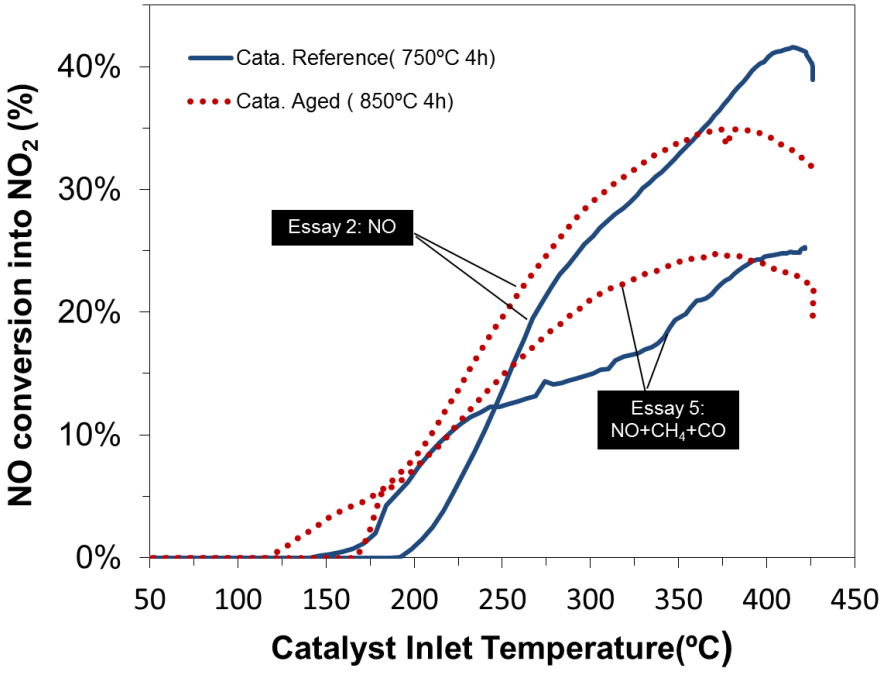

Figure 4.14- Comparison of the NO light-off curves obtained using the reference catalyst (750ºC_4h) and the aged catalyst (850ºC_4h) for essay 1 and essay 5.

Chapter 5: Conclusions

This work was carried out in the Jean Le Rond d' Alembert Institute of Pierre and Marie Curie University, in cooperation with Continental with the purpose of researching the effect of hydrothermal aging on the reactivity and structure of a commercial Diesel Oxidation Catalyst (DOC).

Being the first component exposed to "fresh" diesel exhaust, the DOC experiences more damage than downstream components and besides that increasingly stringed regulations for diesel engine emission have a significant impact on the conditions of operation of DOC. Measures to reduce engine-out NOx and PM, tend to increase CO and HC emissions. Additionally, engine-out NOx reduction is mainly achieved through high amounts of exhaust gas recirculation (EGR) that lower the combustion temperature. All of this, have an impact on the required efficiency of DOC, which has to convert more pollutants at lower temperatures

Lowered DOC oxidation efficiency due to thermal aging effects can lead to reduced NO_2 formation. This potentially influences the efficiency of the exhaust aftertreatment systems downstream of the DOC, including the diesel particulate filter, the NOx storage reduction catalyst, and the selective reduction catalyst.

As mentioned, in this study a commercial catalyst was used, which means that available information about its composition is reduced. For this reason, several characterization techniques were used to identify the physicochemical composition of those catalytic materials, as well as to investigate the effect of the hydrothermal aging on the surface of the catalyst. Furthermore, a correlation between the evolution of the catalyst surface morphology and its catalytic performance, namely in the oxidation of hydrocarbons and NO, after the aging was performed along with the estimation of the interactions effects between the different exhaust gases.

Different structural characterization techniques were performed: textural and morphological proprieties were analyzed by BET and TEM, the characterization of the presented crystallographic phases was performed by DRX and the determination of the number of reducible species was possible by TPR. The characterization of the catalytic performance was carried out on a synthetic gas bench using carrots catalyst under conditions close to the realistic conditions i.e. using a synthetic gas mixture, representative of the exhaust gases from diesel engines, having into account , however the limitations of the apparatus(flows, pressures ,temperatures).

From TEM and DRX results, we conclude that the catalyst support is predominately composed by aluminum and silicon, presented in the form of oxides: alumina (Al_2O_3), which is the main washcoat material and silica (SiO_2) and that, as active components we have a bimetallic complex of palladium and platinum. Globally it was verified that the affinity of the metal particles for the alumina support is greater than their affinity for the aluminosilicate support. TEM results also shown, an increase of the metal particle size with the aging caused by the agglomeration of metal particles, revealing the presence of metal sintering. DRX results suggest the presence of support sintering, nevertheless further analysis would be necessary to prove that. Furthermore, DRX and BET results unexpectedly reveal that the most drastic aging conditions used actually activated the catalyst surface, due to the increase on the available active surface for the oxidation reactions, suggesting an increase in catalytic activity.

From the catalytic activity essays one can conclude that CO has an inhibition effect on methane oxidation, probably due to the competition between CO and CH_4 for Pt/Pd sites. Moreover the presence of NO affects positively methane oxidation conversions, while the presence of methane inhibits the NO oxidation. The explanation for both behaviors may be that NO_2, a product of NO oxidation, is being consumed as an oxidant in CH_4 oxidation reaction, resulting in the appearance of NO oxidation inhibition and hence in an increase of CH_4 conversions. Additionally a relation between the change of slope of the methane light-off curve and the switch between NO_2 and O_2 as an oxidant may have been established. The combined effect of CH_4 and CO led to a further decrease in NO oxidation, for reasons that are not clear. In parallel, the presence of CH_4 and NO improved the CH_4 oxidation conversions, explicable for reasons that seem to be related with the switch between NO_2 and O_2 as an oxidant.

By comparing the light-off curves from the same essays, but using the reference catalyst and the aged catalyst we conclude that the difference between the results for both catalysts, although expected, were not significant which means, that the catalyst has excellent age resistance. Therefore, more drastic aging conditions would be necessary to observe a significant change in the catalyst performance after hydrothermal aging. As expected, the aging affected negatively the catalyst performance on the oxidation of methane and CO, however an improvement of the NO oxidation performance with the aging was observed. Explainable by the fact that the activity of the catalyst for NO oxidation depends on the size of the Pt particle, being that oxidation is better with larger particle size.

Chapter 6: Perspectives

Further work will focus in tree major areas:

- Better comprehension of the effect of aging on the structure of DOC, namely understand if support sintering takes place, through for example, a surface-sensitive quantitative spectroscopic technique - XPS (X-ray photoelectron spectroscopy) analysis and perhaps elementary analysis, to evaluate if a decrease of either aluminum or silicon, the two main components of the support occurs. A pore size distribution study would also be necessary.
- Obtain more significant differences between the aged and the reference catalysts, and for that we have to use a catalyst aged at more severe conditions (850ºC_10h).
- Better understanding of the mechanism behind the observed effect of methane and CO on NO oxidation, for that an essay with NO in the presence of CO should be done. Additionally the effect of NO_2 should be studied, because it perhaps could clarify some aspects related with that mechanism.

Bibliography

[1] A. Russel e W. Epling , “Diesel Oxidation Catalysts,” *Catalysis Reviews: Science and Engineering,* 2011.

[2] E. Lox, D. Lindner, T. Kreuzer e J. Leyrer, “Advanced exhaust gas aftertreatment systems for gasoline and diesel fuelled vehicles,” *Catalysis today,* 1996.

[3] Wards Auto, “World Vehicle Population Tops 1 Billion Units,” [Online]. Available: http://wardsauto.com/ar/world_vehicle_population_110815. [Acesso em March 2014].

[4] International Organization of Motor Vehicle Manufactures(OICA), “World motor vehicle production by country and type”.

[5] F. Haab e H. Fuess, “Structural Characterization of Automotive Catalysts,” *Advanced Engineering Materials,* 2005.

[6] “Lubrizol,” [Online]. Available: https://www.lubrizol.com/EngineOilAdditives/ACEA/ReferenceMaterial/EuropeanUnionEmissionsStandards.html. [Acesso em 2 March 2014].

[7] S. Yea, Y. H. Yapb, S. T. Kolaczkowskib, K. Robinsona e D. Lukyanovb, “Catalyst ‘light-off’ experiments on a diesel oxidation,” *Chemical Engineering Research and Design,* 2012.

[8] H. Dieter Harder, M. Brugger e R. Bruck, “Future SCR NOx after treatment systems for Euro 6”.

[9] A. Manigrasso, “Thèse de doctorat: Modélisations et études de l'impact des évolutions technologiques et normatives sur la catalyse de dépollution Diesel,” 2013.

[10] R. Heck e R. Farrauto, “Automobile exhaust catalysts,” *Applied Catalysis A: General,* 2001.

[11] The international Council on Clean Transportation, “European Vehicle Market Statistics,” 2013.

[12] M. Votsmeir, T. Kreuzer e G. Lepperhoff, “Automobile exhaust control”.

[13] M. Votsmeier, T. Kreuzer e G. Lepperhoff, “Automobile exhaust control,” Wiley-VCH Verlag GmbH & Co. KGaA, 2005.

[14] S. Raux, A. Frobert e E. Jeudy, “Low temperature activity of Euro4 diesel oxidation catalysts: comprehensive material analyses and experimental evaluation of a representative panel,” *Topics in Catalysis ,* 2009.

[15] H. Gandhi, G. Graham e R. McCabe, “Automotive exhaust catalysis,” *Journal of catalysis,* 2003.

[16] C. Bartholomew, “Mechanisms of catalysts deactivation,” *Applied Catalysis A,* 2001.

[17] O. Shakir, A. Yezerets, N. W. Currier e W. S. Epling, “Spatially resolving concentration and temperature gradients during,” Applied Catalysis A: General , 2009.

[18] A. Russel, W. S. Epling, H. Hess, H.-Y. Chen, C. Henry, N. Currier e A. Yezerets, “Spatially-Resolved Temperature and Gas Species Changes in a Lean-Burn Engine,” Ind. Eng. Chem. Res., 2010.

[19] A. Winkler, D. Ferri e M. Aguirre, “The influence of chemical and thermal aging on the catalytic activity of monolithic diesel oxidation catalyst,” *Applied Catalysis B: Environmental,* 2009.

[20] A. K. Neyestanaki, F. Klingstedt, T. Salmi e Y. D. Murzin, “Deactivation of postcombustion catalysts, a review,” *Fuel First,* 2004.

[21] R. Burch e F. Urbano, “Investigation of the Active State of Supported Palladium Catalysts in the Combustion of Methane,” *Applied Catalyses A: General,* vol. 124, pp. 121-138, 1995.

[22] V. Kroger, T. Kanerva, U. Lassi, K. Rahkamaa-Tolonen, T. Lepisto e R. Keiski, “Phosphorus Poisoning of ZSM-5 and Pt/ZSM-5 Zeolite Catalysts in Diesel Exhaust Gas Conditions,” *Topic in Catalysis ,* pp. 42–43 (1–4), 433–436., 2007.

[23] M. Khosravi, A. Abedi, R. Hayes, W. Epling e M. Votsmeir, “Kinetic modelling of Pt and Pt:Pd Diesel oxidation catalysts,” *Applied Catalysis B: Environmental,* 2014.

[24] K. Irani, W. S. Epling e R. Blint, “Effect of hydrocarbon species on no oxidation over diesel oxidation catalysts,” *Applied Catalysis B: Environmental,* 2009.

[25] S. Katare, J. Patterson e P. Laing, “Aged DOC is a net consumer of NO2: analysis of vehicle engine dynamometer and reactor data,” *SAE Techical Papers ,* 2007.

[26] Kim, Young-Deuk; Jeong, Soo-Jing; Kim, Woo-Seung, “Optimal design of axial noble metal distribution for improving dual monolithic,” *Chemical Engineering Science,* 2009.

[27] V. Cominos e A. Gavriilidis, “Theoretical investigation of axially non-uniform catalytic monoliths for methane combustion,” *Chemical Engineering Science,* vol. 56, pp. 3455-3468, 2001.

[28] S. Oh e J. Cavendish, “Transients of monolithic catalytic converters: response to step changes in feed stream temperature as related to controlling automobile emissions,” *Industrial and Engineering Chemistry Product Research and Development ,* vol. 21, p. 29–37., 1982.

[29] V. Khanaev, E. Borisova e A. Noskov, “Optimization of the active component distribution through the catalyst bed for the case of adiabatic reactor,” *Chemical Engineering Science,* vol. 60, pp. 5792-5802, 2005.

[30] N. T. Inc., “http://www.nettinc.com/information/emissions-faq/how-does-an-oxidation-catalyst-work,” [Online]. [Acesso em 09 2014].

[31] N. C. L. C. G. B. D. Z. W. D. W. E. F. R. S.S. Mulla, “Reaction of NO and O"2 to NO"2 on Pt: Kinetics and catalyst deactivation,” *Journal of Catalysis ,* vol. 241 , pp. 389-399, 2006.

[32] R. Farrauto, M. Hobson, T. Kenely e E. Waterman, “Catalytic chemistry of supported palladium for combustion,” *Applied Catalysis A: General,* 1991.

[33] A. Manigrasso, N. Fouchal e P. Da Costa, “Hysteresis study on diesel oxidation for better efficiency of SCR systems,” *Catalysis Today,* 2012.

[34] M.Khosravi, C.Sola, A.Abedi, R.E.Hayes, W.S.Epling e M.Votsmeir, “Oxidation and selective catalytic reduction of NO by propene over Ptand Pt:Pd diesel oxidation catalysts,” *Applied Catalysis B: Environmental,* vol. 147, pp. 264-274, 2014.